

Decadal nitrogen addition alters chemical composition of soil organic matter in a boreal forest



Shun Hasegawa^{a,*}, John Marshall^a, Tobias Sparrman^b, Torgny Näsholm^a

^a Department of Forest Ecology and Management, Swedish University of Agricultural Sciences, Umeå, Sweden

^b Department of Chemistry, Umeå University, Sweden

ARTICLE INFO

Handling Editor: Ingrid Kögel-Knabner

Keywords:

Boreal forest
 Soil organic matter
 Nitrogen enrichment
 Carbon accumulation
 Pyrolysis
 NMR

ABSTRACT

Boreal forests store approximately 470 Pg of carbon (C) in the soil, and rates of soil C accumulation are significantly enhanced by long-term nitrogen (N) enrichment. Dissecting the compositional profile of soils could help better understand the potential mechanisms driving changes in C cycling under enriched N conditions.

We examined the impacts of long-term N addition on the chemical composition of soil organic matter (SOM) in a mature boreal forest. Two large experimental plots (15 ha each) were established: a control and a fertilised plot. The latter received NH₄NO₃ fertilizer at an average rate of 75 kg N ha⁻¹ year⁻¹ for 12 years. While the centre of this plot received the prescribed amounts of fertilizer, the year-to-year variation in distribution of fertilizer around the designated edges of the plot created a gradient in N-loading. Along this gradient, a compositional shift in SOM in the organic horizon was assessed using two methods: pyrolysis-gas chromatography/mass spectrometry (GC/MS) and solid-state ¹³C nuclear magnetic resonance spectroscopy (¹³C NMR).

Both of these methods revealed that the chemical composition of SOM changed with increasing N loading, with an increased fraction of lignin derivatives (i.e., aromatic, methoxy/N-alkyl C) relative to that of carbohydrate (i.e., O-alkyl C), accompanied by increased soil C mass (kg m⁻²) at the fertilised plot. Also, the relative abundance of N compounds in the pyrolysis products increased with the N loading, mainly due to increased methyl N-acetyl- α -D-glucosaminide in the F/H horizon, plausibly of microbial origin. Microbial N processing likely contributed to soil accumulation of fertilizer-derived N.

Our results corroborate the hypothesis that addition of inorganic N suppresses enzymatic white-rot decomposition relative to non-enzymatic brown-rot oxidation. Taken together, our study suggests that N enrichment leads to a selective accumulation of lignin-derived compounds and points to a key role of such compounds for N-induced SOM accumulation.

1. Introduction

The importance of soil organic matter (SOM) as a carbon (C) sink has long been recognised (Batjes, 1996) as soils store as much as, or more C than, that in the combined atmosphere and vegetation (IPCC, 2013). Thus, even a small change in SOM will have vast impacts on global C cycling and therefore it is essential to scrutinise the impacts of climate and environmental perturbation on SOM in forests (Kirschbaum, 2000). The amount of SOM sequestered is determined by the balance of input and output of C. Cell walls in plant residues, composed of a complex of lignin, cellulose and hemicellulose known as lignocellulose, are a principal source of soil C in the organic horizon in forest ecosystems (Kögel-

Knabner, 2002; Tarasov et al., 2018). This C is primarily lost from the system as inorganic C (i.e., carbon dioxide; CO₂) via decomposition (or mineralisation), with a variable yet often relatively small fraction lost as a leachate in a dissolved form (Guggenberger et al., 1994; Öquist et al., 2014).

The long-term use of fertilizers for both agricultural and forestry purposes as well as atmospheric nitrogen (N) deposition resulting from combustion of fossil fuels have been adding significant quantities of N to many terrestrial ecosystems since the industrial revolution (Davidson, 2009; Galloway et al., 2008). This N-load has led to an altered C:N balance in terrestrial biomes (Dignac et al., 2002; Yang et al., 2011). As N fluxes are intimately coupled with C fluxes in terrestrial systems, the

* Corresponding author at: Department of Forest Ecology and Management, Swedish University of Agricultural Sciences, SE-901 83 Umeå, Sweden.

E-mail addresses: hasegawa.shun.skg@gmail.com (S. Hasegawa), john.marshall@slu.se (J. Marshall), tobias.sparrman@umu.se (T. Sparrman), torgny.nasholm@slu.se (T. Näsholm).

altered input of N also most probably has influenced soil C cycling. The impacts of long-term N enrichment on C cycling, especially C accumulation, has been examined in numerous studies during the past few decades (e.g., Fog, 1988; Reay et al., 2008). Whilst contrasting results have been reported, a majority of studies suggest N enrichment of temperate and boreal forests increases C sequestration due to suppressed SOM decomposition (e.g., Berg and Matzner, 1997; Hyvönen et al., 2008; Janssens et al., 2010; Liu and Greaver, 2010; Zak et al., 2017) and, to a lesser extent, due to enhanced forest productivity and consequently increased litter inputs (e.g., Forsmark et al., 2020). A few potential mechanisms for the suppressed decomposition have been suggested to date. For instance, some reports argue that increased N availability hampers microbial ligninolytic activity via suppression of oxidative enzymes (Maaroufi et al., 2015; Waldrop et al., 2004; Waldrop and Zak, 2006), increases microbial residues that are relatively less decomposable (Clemmensen et al., 2013; Frey et al., 2014) and/or facilitates physical protection of soil particles from decomposition (Zak et al., 2017). Additionally, soil acidification induced by N addition is reported to suppress microbial activity and lead to formation of mineral associated C, retarding SOM decomposition (Ye et al., 2018). Nonetheless, the contribution of each suggested mechanism to SOM accumulation remains largely uncertain due to the complexity of both the formation and the decomposition of SOM (Hättenschwiler et al., 2005).

Bonner et al. (2019), in line with reasoning by Fog (1988), postulated a mechanism by which N enrichment would suppress SOM decomposition via an altered balance of competition over energy gain between typical phenotypes of lignocellulose decomposing saprotrophs: white-rotters vs. brown-rotters. The former produce lignin-oxidative enzymes and thereby have the potential to fully decompose lignocellulose complexes. The latter employ non-enzymatic oxidation with hydroxy radicals produced through Fenton chemistry and modify lignin so that cellulose and hemicellulose can be decomposed. The latter reaction results in the preservation of modified, yet non-mineralised, lignin (Goodell et al., 1997; Hatakka and Hammel, 2011). Bonner et al. (2019) suggested that N addition would make white-rot activity less efficient and cause the competitive balance to shift towards the brown-rot activity. The proposed mechanism is in line with the well-documented observations in enzymology in which N addition suppresses ligninolytic enzymes (Chen et al., 2018, 2019; Frey et al., 2004; Rinkes et al., 2016; Zak et al., 2019) while enhancing cellulolytic enzyme activity (Allison et al., 2008; Frey et al., 2004; Stark et al., 2014).

Despite the plethora of studies on N addition and SOM decomposition, only a limited number of studies have examined the whole profile of chemical composition in soils under enriched N conditions using comprehensive approaches like pyrolysis-gas chromatography/mass spectrometry (GC/MS) and nuclear magnetic resonance spectroscopy (NMR). Those that have utilised these methods were mainly targeting forest ecosystems of the temperate region (e.g., Feng et al., 2010; Frey et al., 2014; Grandy et al., 2008; Pisani et al., 2015). In contrast, relatively little is known about belowground responses of boreal forests to N addition despite the significant contribution of boreal soils, c. 470 Pg C, to the global C stock (Deluca and Boisvenue, 2012; Lal, 2005; Malhi et al., 1999). Here, we report on a study using a long-term (12 years) N-fertilisation experiment established in a mature Scots pine (*Pinus sylvestris*) forest in northern Sweden and investigate the chemical composition of SOM using two methods: pyrolysis GC/MS and solid-state ¹³C NMR (¹³C NMR). The study aimed at testing the above-mentioned hypothesis that N enrichment would lead to soil C-enrichment by favouring the preservation of lignin-derived C (e.g., aromatics, phenolic compounds) in SOM. Additionally, we tested the hypothesis that N enrichment would lead to an increase in the fraction of aliphatic compounds derived from plant tissues (e.g., cutin, suberin) and/or microbial-derived compounds (e.g., chitin, acetamides, *N*-acetylglucosamine) owing to accumulated microbial residues (Lenardon et al., 2010; Poirier et al., 2005; Stankiewicz et al., 1996; Stuczynski et al., 1997). The study was performed as a part of a comprehensive investigation of

the effects of N supply on ecosystem C fluxes using eddy covariance and compartmental fluxes.

2. Materials and methods

2.1. Study site

This study was carried out at the Rosinedalsheden Experimental Forest, situated c. 60 km northwest of Umeå, Sweden (64°10'N, 19°45'E, 145 m a.s.l.; Fig. 1a), where the background atmospheric N deposition is c. 2 kg N ha⁻¹ year⁻¹ (Pihl-Karlsson et al., 2013). The mean annual temperature is 1.2 °C and the mean annual precipitation is 520 mm, with snow cover between October and May (Swedish Meteorological and Hydrological Institute, <https://www.smhi.se/>). The soil is podzol of glacial till with texture of fine sand and silt. Our study was conducted as a part of the long-term, large-scale experiment that aimed to assess ecosystem-scale C fluxes in a mature Scots pine forest using the eddy-covariance technique. Two large experimental plots of c. 15 ha each were established 2 km apart from one another, laid on a flat topography. A flux tower was installed in the centre of each plot. One of the plots received NH₄NO₃ granule fertilizer in June at a rate of 100 kg N ha⁻¹ year⁻¹ between 2006 and 2011 and 50 kg N ha⁻¹ year⁻¹ in 2012 and thereafter. This resulted in a total amount of added N of 950 kg ha⁻¹ by 2018. The other plot received no fertilizer. Although unreplicated due to financial and operational limitations of eddy-covariance studies, the exceptionally large size of these experimental plots compared to many other N-manipulation experiments would provide valuable empirical data on ecosystem processes, together with the eddy covariance study. The overstorey vegetation is a homogeneous tree stand of c. 90-year-old *Pinus sylvestris* L. (Scots pine) at a tree density of 888 trees ha⁻¹. Both of the two experimental plots had experienced the same history of forest management until the commencement of the study in 2006, in which the tree stands had been naturally regenerated in 1920–1925 from the soil seed bank following a fire event and thinned in 1955, 1976 and 1993. The understorey is dominated by two dwarf shrub species of *Vaccinium*: *V. myrtillus* L. (bilberry) and *V. vitis-idaea* L. (lingonberry). The forest floor is covered by moss (*Pleurozium schreberi* (Brid.) and *Hylocomium splendens* (Hedw.) Schimp) with a small proportion of lichen (*Cladonia* spp.; Hasselquist et al., 2012).

2.2. Transect establishment

The fertilizer was applied to the plot at the fertilised treatment using a helicopter, resulting in somewhat variable distribution of the fertilizer near the edges of the plot. Thus, although the centre of the plot received the prescribed amounts of fertilizer, the year-to-year variation in distribution of fertilizer around the designated edges of the fertilised plot created a gradient in N-loading. This created an opportunity for us to study how variable rates of N addition will affect SOM chemical composition. Transects were established so that they crossed over the edge perpendicularly on the southwestern side of the fertilised plot, capturing the high and low ends of N-loading (Fig. 1a). Five 200 m-long transects were established, 50 m apart from one another. Half of each transect was situated within the theoretical border of the fertilised plot and the other half outside the boarder. The outermost transects were more than 100 m away from the nearest corners of the fertilised plot. Sampling plots (2 × 2 m) were established along each transect: one on the theoretical edge of the fertilised plot and four at a distance of 10, 30, 60 and 100 m from this edge towards both inside and outside of the fertilised plot, resulting in nine sampling plots in each transect. The same scale of transects was established in the control plot, in which there were five transects 50 m apart from one another, within each of which six to seven 2 × 2 m sampling plots were established >30 m away from the next ones. There were 45 and 32 sampling plots at the fertilised and control plots, respectively.

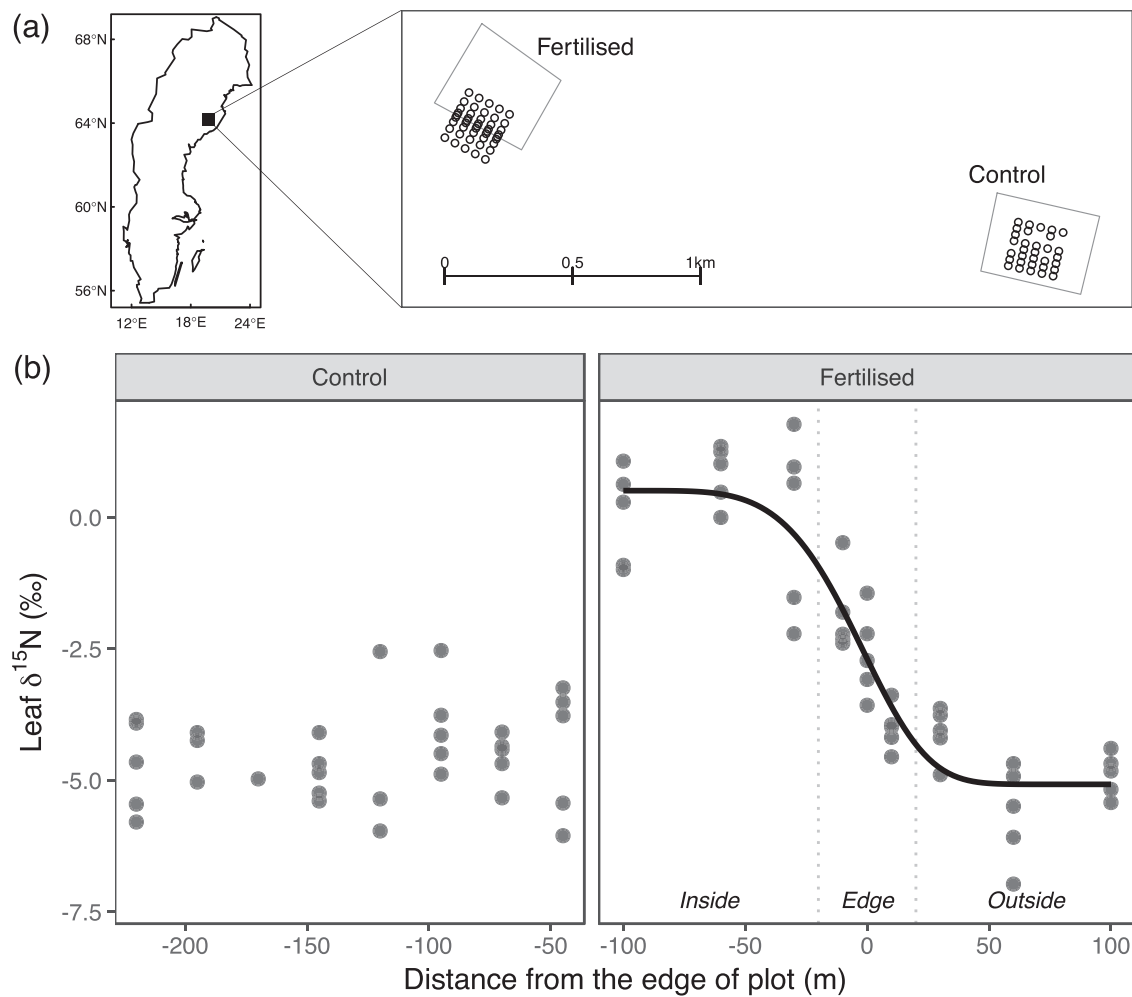


Fig. 1. a) A map of the experimental site and transect design of sampling plots depicted by circles. b) $\delta^{15}\text{N}$ of the *Vaccinium vitis-idaea* leaves as a function of distance from the designated edge of plots (Distance = 0) towards the centre of the plot (Distance < 0) and outwards (Distance > 0). The fertilised plot is categorised into three groups: Inside (Distance < -10 m), Edge (-10 m ≤ Distance ≤ 10 m) and Outside (Distance > 10 m). A four-parameter S-shaped asymptotic regression line was fitted to the values from the fertilised treatment using the extended Weibull model: $y = -5.07 + 5.58e^{-e^{-22.03}(x+101)^{4.74}}$

2.3. Gradient of N-loading

Our approach was to use the gradient in N-loading resulting from the year-to-year variation in distribution of fertilizer around the theoretical edge of the fertilised plot. Characterization of the N-load at each $2 \times 2\text{ m}$ sampling plot therefore became a central element of the study. A previous study conducted in *Picea abies* (Norway spruce) and Scots pine forests nearby our study site (<10 km) demonstrated that leaf N concentrations of *V. vitis-idaea* increased with the amount of N added to the experimental sites (Palmroth et al., 2014). Furthermore, Hobbie et al. (2019) measured the relative abundance of the stable N isotope ^{15}N ($\delta^{15}\text{N}$) in the mineral fertilizer that had been applied to our study site using the same technique as described below (Section 2.5), reporting it to be $1.9 \pm 0.1\%$ (mean \pm 1 standard error, $n = 5$); the $\delta^{15}\text{N}$ of the fertilizer was found more enriched relative to that of the N in the unfertilised soil (-1.44 ± 0.48 , $-0.60 \pm 0.50\%$ in the L and F/H horizons, respectively, mean \pm 95% confidence interval, $n = 11$, also see the Section 2.5), which provided a second proxy for assessing N-loading at plot scale. Thus, two metrics of *V. vitis-idaea* leaves could be used to assess the historical N-loading of each $2 \times 2\text{ m}$ sampling plot: %N and $\delta^{15}\text{N}$ in *V. vitis-idaea* leaves. Based on preliminary data, we used the latter metric in each of the sampling plots. Analysis of *V. vitis-idaea* leaves (see the Section 2.5) revealed a decrease in $\delta^{15}\text{N}$ as sampling locations became more distant from the centre of the fertilised plot,

whereas no such pattern was seen in the control plot (Fig. 1b). Thus, leaf $\delta^{15}\text{N}$ in *V. vitis-idaea* represented the gradient of N-loading created by uneven application of the fertilizer adjacent to the designated edge of the fertilised plot, providing a unique opportunity to assess a trajectory of SOM shift along the environmental gradient. *Vaccinium vitis-idaea* occurred in every sampling plot at the study site, allowing us to capture the between-plot variation in N-loading. Based on the gradient of leaf $\delta^{15}\text{N}$, the sampling plots from the fertilised treatment were further categorised into three location groups: edge (within 10 m from the edge of the plot), inside (>10 m away from the edge towards the centre of the fertilised plot) and outside (>10 m away from the edge outwards from the fertilised plot; Fig. 1b). Here, the measurements taken in our study will be summarised according to these location groups to present data variability.

2.4. Soil and leaf sampling and processing

Soil sampling was conducted in October 2018 after 12 years of fertilisation. Of the 32 sampling plots at the control treatment, soil samples were collected from 11 randomly selected plots, whereas soils were collected from all of the 45 plots at the fertilised treatment ($n = 56$). Within each $2 \times 2\text{ m}$ sampling plot, three locations were randomly chosen where $10 \times 10\text{ cm}$ of the organic horizon was cut out of the soil above the mineral layer. The resulting three clipped organic soil profiles

were bulked together into a resealable plastic bag per sampling plot. On the day of sampling, the soil samples were brought back to a laboratory and thoroughly dried at 40–50 °C in a drying oven for over a week. The dried-samples were 2 mm-sieved, separated into two groups: large plant materials and soil particles. The former was mainly composed of plant residues (e.g., needles, twigs and roots), hence referred to as the “L-horizon”, whilst the latter was composed of the mixture of small particles of fragmented plant-derived matters and humus soil, referred to as the “F/H-horizon”. Subsamples were taken for each sample in each horizon and ground to a fine powder, prior to further analyses described in the sections below. The L-horizon was chopped so that its particle size was <1 cm and homogenised well prior to subsampling. The samples from L- and F/H-horizons were ground with a tube mill (IKA Tube Mill control) and ball mill, respectively. At the time of soil sampling, the leaves of *V. vitis-idaea* were collected from all the sampling plots ($n = 77$). The live moss layer was also collected directly above each of the three clipped organic soil profile described above and bulked per sampling plot ($n = 55$). The *V. vitis-idaea* leaves and moss were dried in an oven at 80 °C for 3–4 days and finely ground using a ball mill and a tube mill, respectively. Dry weight of moss was recorded to calculate area-based C mass.

2.5. Isotope ratios mass spectrometer (IRMS)

The ground samples of soils, leaves and moss were analysed for $\delta^{15}\text{N}$ as well as %C and %N at the Swedish University of Agricultural Sciences Stable Isotope Laboratory (Umeå, Sweden), using a Flash 2000 Elemental Analyzer attached to a Delta V Advantage Isotope Ratio Mass Spectrometer (Thermo Fisher Scientific, Bremen, Germany).

2.6. Pyrolysis gas-chromatography/mass spectrometry (GC/MS) analysis

The initial pyrolysis GC/MS conditions were set up following Gerber et al. (2012). Briefly, an oven pyrolyser was connected to the GC/MS system (Agilent, 7890A-5975C, Agilent Technologies AB, Sweden), equipped with an autosampler (PY-2020iD and AS-1020E, Frontier Laboratories, Japan). The pyro-gas was injected with a carrier gas of helium at a ratio of 1:16. A DB-5MS capillary column was used (30 m long, 0.25 mm diameter and 0.25 μm film thickness; J&W, Agilent Technologies AB, Sweden). Sample volume, pyrolysing temperature and scan mass spectra were optimised following Tolu et al. (2015). Soil samples of 110 and 120 μg ($\pm 10\%$) were weighed into autosampler containers (Eco-cup SF, Frontier Laboratories, Japan) on an analytical balance (XP6, Mettler-Toledo, Zaventem, Belgium) for the L- and F/H-horizon samples, respectively, determined based on their soil C contents. The pyrolysing temperature was 450 °C. The scanned range of mass spectra were between 30 and 500 mass to charge ratios (m/z) so that long-chain C molecules and steroids could be captured (Tolu et al., 2015). Peaks of mass spectra generated from the MS were detected by Chemstation (Agilent Technologies AB, Sweden). The GC temperature was initially 40 °C, raised step-by-step to 1) 100 °C at a rate of 32 °C min^{-1} , 2) 120 °C at 6 °C min^{-1} , 3) 250 °C at 15 °C min^{-1} , and finally 4) 320 °C at 32 °C min^{-1} .

2.7. Pyrolysis data processing

The pyrolysis data were processed for peak integration and extraction of their mass spectra following Jonsson et al. (2005) and Tolu et al. (2015). Here, we describe this data processing briefly, but consult the original papers for details. First, the chromatogram generated from the pyrolysis was exported in AIA format. The AIA data were processed using R 2.15.2 (R Core Team, 2012) by a hierarchical multivariate curve resolution approach following Jonsson et al. (2005); thereby the chromatogram was processed for smoothing, alignment and background correction. It resulted in 1) chromatogram peak position with area size and 2) their mass spectra. The resulting mass spectra were imported into

NIST (NIST MS Search 2.0), in which molecular compounds were assigned based on peak heights and positions of mass spectra. Several possible candidates were often suggested by NIST for each chromatogram peak, and hence the most likely one was selected based on retention time reported in other studies that analysed soils, sediments or plant materials (Abelenda et al., 2011; Buurman et al., 2009; Schellekens et al., 2009; Tolu et al., 2017). As a result of the data processing and NIST analysis, 91 compounds were assigned for the L-horizon out of 273 chromatogram peaks, accounting for 68.2% of the total area of the chromatogram including CO₂ (17.6%; Table S1). For the F/H-horizon samples, 72 compounds were identified out of 205 chromatogram peaks, responsible for 74.3% of the total area of the chromatogram including CO₂ (19.3%; Table S2). The assigned compounds of the pyrolysis products (pyrolysates) were categorised into the following groups and peak areas were integrated for each: carbohydrate, guaiacyl lignin (g-lignin), N compounds, phenolic compounds, syringyl lignin (s-lignin), other aromatic derivatives, other aliphatic derivatives (fatty acid, ketone, alkane and alkene) and others (steroid, vitamin, chlorophyll and hopanoid). Following a removal of the chromatogram peaks of CO₂ and the unknown, relative abundance of peak area (%) of those categories were computed for each soil sample in each horizon.

2.8. Solid-state ^{13}C nuclear magnetic resonance (^{13}C NMR)

All solid-state NMR spectra were acquired using a Bruker Avance III 500 MHz spectrometer equipped with a 4 mm HX CP MAS probe and a SamplePro HR-MAS sample changer. Experiments were recorded at a magic angle spinning (MAS) rate of 10 kHz and at a temperature of 298 K. The cross-polarization (CP) experiments used a 90° excitation pulse of 3 μs for ^1H , followed by a contact time of 1.5 ms with a ^{13}C spin lock frequency of 60 kHz while ^1H was ramped from 45 up to 90 kHz. ^1H decoupling with a “spinal64” decoupling scheme at 83 kHz was applied during the acquisition (Fung et al., 2000). The repetition delay was set to 2 s and 4000 scans were acquired for each sample. The chemical shift scale was externally referenced to the adamantane CH₂ signal at 38.48 ppm (Morcombe and Zilm, 2003). Functional groups were assigned to the following seven chemical shift regions of NMR spectra (Smernik, 2005): carbonyl C (190–160 ppm), O-aromatic C (160–140 ppm), aromatic C (140–112 ppm), di-O-alkyl C (112–93 ppm), O-alkyl C (93–60 ppm), methoxy/N-alkyl C (60–50 ppm) and alkyl C (50–0 ppm). Relative contribution to the total area of NMR spectra at 190–0 ppm was computed for each region. Carbonyl C originates from lipids and amino acids. O-aromatic and aromatic C are derived from lignin and tannin compounds. Di-O-alkyl C is derived from cellulose, tannin and lignin compounds while O-alkyl C is derived from carbohydrate compounds. Methoxy/N-alkyl C originates from lignin or protein compounds. Alkyl C can be derived from fatty acids, and surface waxes and cutin on leaves (Harrysson Drotz et al., 2010 and references therein).

2.9. Statistical analysis

This study was conducted as a part of the ecosystem-scale C flux measurement experiment using the eddy-flux technique as mentioned above. Our study shared a common limitation of all eddy-flux studies—no replication. Instead of comparing observations between the control and fertilised plots, we assessed the association between the observed values and the gradient of N-loading resulting from a decade of high-intensity N application (Fig. 1). This allows us to evaluate the driver of trajectory changes in the soil measurements (e.g., SOM chemical composition, lignin:carbohydrate ratios) along the N level, given that the two study plots were sufficiently large (c. 15 ha) and laid on a flat topography, with spatially homogeneous vegetation and soil texture (Hasselquist et al., 2012; Lim et al., 2015). Statistical analysis was performed using R 3.5.2 (R Core Team, 2018). Herein, we report statistically significant results at $\alpha = 0.05$.

Redundancy analysis (RDA) was employed to assess a shift in

chemical composition of SOM with the N gradient—evaluated by leaf $\delta^{15}\text{N}$ in *V. vitis-idaea*—for each of pyrolysis- and NMR-products ($n = 56$), performed using the ‘vegan’ package (Oksanen et al., 2018). Proportional data of organic compounds were Hellinger-transformed prior to RDA. RDA was tested using a permutation test (4999 permutations) with pseudo- F given by the ratio of constrained and unconstrained total Inertia (Legendre and Legendre, 2012; Oksanen et al., 2018). The RDA analysis with leaf $\delta^{15}\text{N}$ was also performed on a subset of data obtained only from the sampling plots at the inside, edge and outside of the fertilised treatment ($n = 45$) without including those from the control treatment to evaluate whether the variation observed in a complete dataset was due to the difference between two sampling sites (i.e., control vs. fertilised plot) or the N gradient.

Linear mixed-effects models were performed using the ‘lme4’ package (Bates et al., 2015) to examine the effects of the N level on the ratios of lignin to carbohydrate compounds in the pyrolysates (lignin: carbohydrate) under two different horizons, with sampling plot as a random factor. The abundance of lignin compounds was obtained by the sum of g-lignin, s-lignin and phenolic compounds. Also, the ratios of g-lignin to s-lignin in the pyrolysates (G/S-lignin) were analysed in the same manner to assess the contribution of gymnosperm (e.g., Scots pine) and angiosperm (e.g., *V. vitis-idaea*) species to the litter inputs as the lignin from the former group primarily yields g-lignin while that from the latter resulting in both g- and s-lignin (Sarkanen and Ludwig, 1971). The response variables in the linear-mixed effects models were transformed (inverse or log_e) to ensure homogeneity of variances and normality of errors prior to the analysis where necessary (Crawley, 2012; Fox and Weisberg, 2011). P values of the fixed factors were approximated by F-test using Type II ANOVA tests with Kenward-Roger

Degrees of Freedom using the “car” and “lmerTest” packages (Fox and Weisberg, 2011; Kenward and Roger, 1997; Kuznetsova et al., 2017). Person’s correlation test was performed for each horizon separately to examine the relationship between relative abundance of N compounds obtained from the pyrolysis and leaf $\delta^{15}\text{N}$ and between lignin:carbohydrate ratios and soil C mass (kg C m^{-2}). Lignin:carbohydrate ratios were inverse-transformed prior to the correlation test.

3. Results

3.1. Pyrolysis

The pyrolysates were mainly attributed to carbohydrate-derived compounds, responsible for more than a half of identified compounds in both of the L and F/H horizons (Figs. 2, S1–8). Relative abundance of carbohydrate-derived compounds consistently decreased with increasing $\delta^{15}\text{N}$ from 66.3% at the control to 54.3% at Fertilised:inside conditions in the L-horizon and from 65.3% to 59.1% in the F/H-horizon, respectively. The carbohydrate fraction was mainly derived from levosugars, anhydro-sugars and butyraldehyde (Fig. S1). G-lignin was second-dominant in the pyrolysates in this study, whose relative abundance increased with increasing $\delta^{15}\text{N}$ at the expense of that of carbohydrate from 19.1% at the control to 28.8% at Fertilised:inside in the L-horizon and from 14.9% to 19.0% in the F/H-horizon, respectively (Fig. 2).

The contribution of N compounds to the total pyrolysates was relatively small compared to that of carbohydrate or g-lignin, accounting for c. <1% and 2% in the L- and F/H-horizons, respectively (Fig. 2). Nevertheless, the relative abundance of N compounds was significantly,

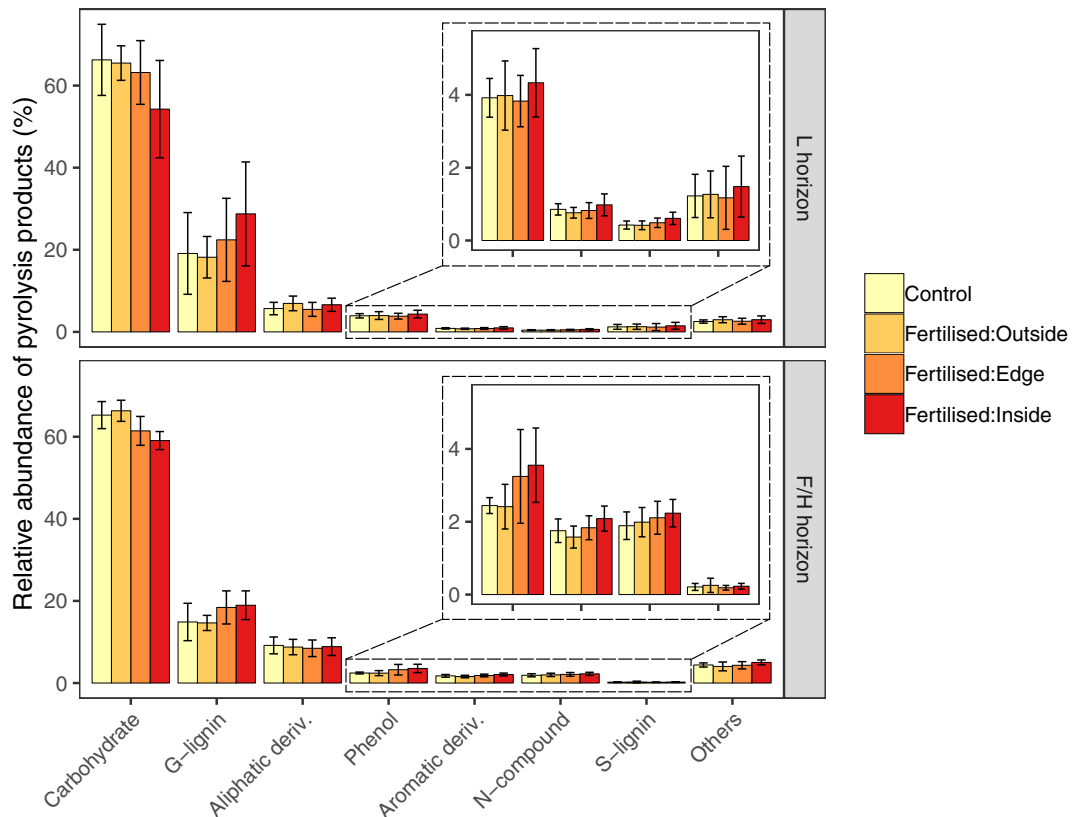


Fig. 2. Relative abundance (%) of pyrolysis products in the L- and F/H-horizons (Mean \pm 1 standard deviation): carbohydrate, guaiacyl lignin (g-lignin), aliphatic derivatives (aliphatic deriv.: fatty acid, ketone, alkane and alkene), phenolic compounds (phenol), other aromatic derivatives (aromatic deriv.), N compounds (N-compound), syringyl lignin (s-lignin), and others (steroid, vitamin, chlorophyll and hopanoid). See Table S1 and S2 for the full list of identified compounds. In addition to the control plot ($n = 11$), sampling plots in the fertilised plot were further categorised into three groups: inside (>10 m inwards from the edge, $n = 15$), edge (≤ 10 m from the edge, $n = 15$) and outside (>10 m outwards from the edge, $n = 15$) (also see Fig. 1). The results for phenol, aromatic deriv., N-compound and s-lignin are enlarged, shown in subpanels.

positively associated with leaf $\delta^{15}\text{N}$ in both of the L-horizon ($P < 0.001$, $df = 54$, $r = 0.43$) and the F/H-horizon ($P < 0.05$, $df = 54$, $r = 0.29$). Dominant N-compounds slightly differed between the L- and F/H-horizons (Fig. S3). In the L-horizon, the N compound fraction was mainly composed of cyclo proline-proline (Pro-Pro) and diketodopyrrole. For the F/H-horizon, while cyclo (Pro-Pro) was also observed, the N compound was mainly composed of methyl N -acetyl- α -D-glucosaminide and pyrrole/pyridine.

3.2. ^{13}C NMR

The NMR-products were mainly comprised of O-alkyl C (40% and 34%) and alkyl C (21% and 30%) in the L- and F/H-horizons, respectively (Fig. 3). O-aromatic, aromatic and methoxy/N-alkyl C were generally considered to be lignin- or protein-related (Harrysson Drotz et al., 2010; Nelson and Baldock, 2005 and references therein), altogether accounting for 24% and 22% in the L- and F/H-horizons, respectively (Fig. 3).

3.3. A shift in chemical composition of SOM along the N gradient

Redundancy analysis revealed a significant association between the chemical composition of SOM and *V. vitis-idaea* leaf $\delta^{15}\text{N}$ for both the pyrolysates and NMR-products in both the L- and F/H-horizons. Site scores of the RDA axes for the pyrolysates and NMR-products were plotted together alongside corresponding species loadings to visualise the whole pattern of the shift in chemical composition of SOM (Fig. 4). For the L-horizon, there was a significant association between leaf $\delta^{15}\text{N}$ and chemical composition of pyrolysates ($\text{pseudo-}F_{1, 54} = 15.51$, $P < 0.001$) and of NMR-products ($\text{pseudo-}F_{1, 54} = 6.52$, $P < 0.01$, Fig. 4a). The RDA axes explained 22.3% and 10.8% of the total variability in the

chemical composition for the pyrolysates and NMR-products, respectively. The chemical composition gradually shifted from the top-right to the bottom-left corner of the ordination plot as the N level increased (Fig. 4a). The species loadings suggest that pyrolysis-RDA1 was positively driven by carbohydrate and negatively by g-lignin fractions and that NMR-RDA1 was positively driven by O-alkyl and di-O-alkyl C and negatively by methoxy/N-alkyl and aromatic C fractions, respectively. For the F/H-horizon, there was a significant association between leaf $\delta^{15}\text{N}$ and chemical composition of pyrolysates ($\text{pseudo-}F_{1, 54} = 13.83$, $P < 0.001$) and of NMR-products ($\text{pseudo-}F_{1, 54} = 6.98$, $P < 0.01$, Fig. 4b). The RDA axes explained 20.4% and 11.4% of the total variability in the composition for pyrolysates and NMR-products, respectively. A similar pattern to that of the L-horizon emerged, demonstrating a shift in chemical composition of SOM from the top-right to the bottom left of the ordination plot as leaf $\delta^{15}\text{N}$ increased (Fig. 4b). Pyrolysis-RDA1 was positively driven by carbohydrate and negatively with g-lignin and phenol fractions. NMR-RDA1 was positively driven by O-alkyl and di-O-alkyl C and negatively by aromatic and methoxy/N-alkyl C.

The RDA analysis demonstrated that pyrolysis and ^{13}C NMR consistently provided a general pattern in the shift of chemical composition for both of the L- and F/H-horizons. Whilst a higher fraction of carbohydrate (O-alkyl in ^{13}C NMR) was observed under the non-fertilised plot, a higher fraction of lignin (esp. g-lignin, methoxy- or aromatic-C in ^{13}C NMR) was observed in the fertilised plot. Despite the above-mentioned significant correlation between the N compound fraction in the pyrolysates and leaf $\delta^{15}\text{N}$, its contribution to the pyrolysis-RDA1 appeared small compared to that of g-lignin and carbohydrate (Fig. 4). When a subset of data obtained only from the sampling plots at the inside, edge and outside of fertilised plot was analysed in the same manner without those from the control plot, there was still a significant association between chemical composition and leaf $\delta^{15}\text{N}$ for

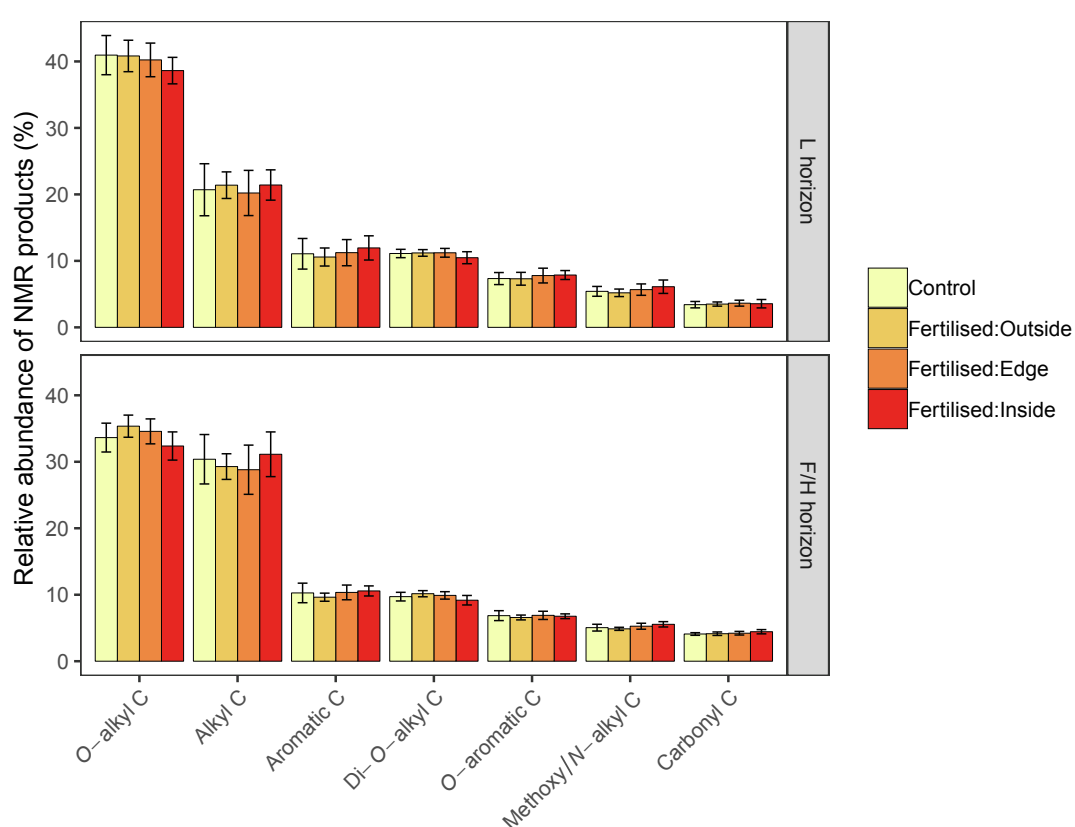


Fig. 3. Summary of relative abundance (%) of the products of solid-state ^{13}C nuclear magnetic resonance spectroscopy (^{13}C NMR) in the L- and F/H-horizons (Mean \pm 1 standard deviation.). In addition to the control plot ($n = 11$), sampling plots in the fertilised plot were further categorised into three groups: inside (> 10 m inwards from the edge, $n = 15$), edge (≤ 10 m from the edge, $n = 15$) and outside (> 10 m outwards from the edge, $n = 15$) (also see Fig. 1).

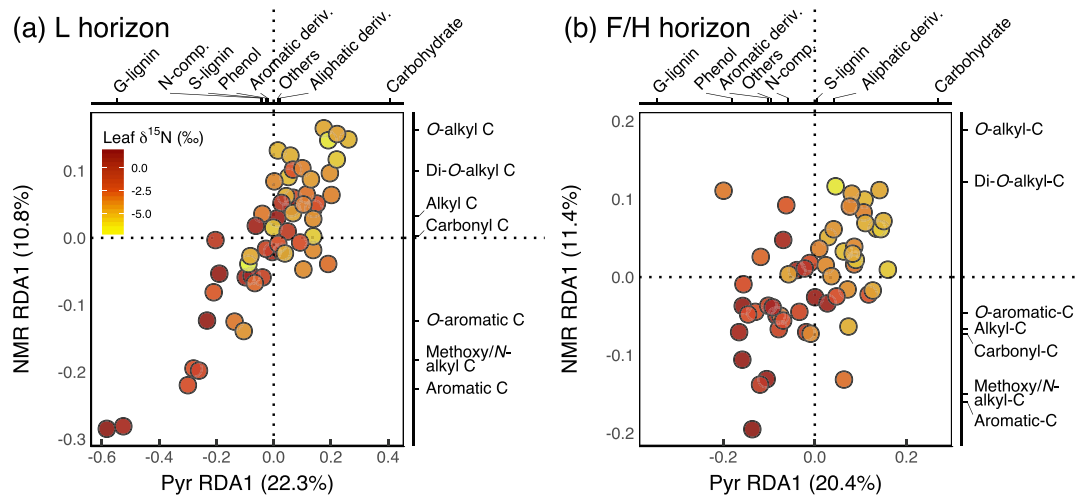


Fig. 4. Plots depicting the association between the chemical composition of soil organic matter (SOM) obtained by pyrolysis GC/MS and ^{13}C NMR products in a) the L-horizon and b) the F/H-horizon, with concomitant changes in $\delta^{15}\text{N}$ of *Vaccinium vitis-idaea* leaves. Each axis is obtained from the site scores of redundancy analysis (RDA) performed on changes in chemical composition with leaf $\delta^{15}\text{N}$ for each of the pyrolysis GC/MS (Pyr RDA1) and ^{13}C NMR (NMR RDA1), presented with corresponding species loadings of compound types alongside. The site scores and species loadings are scaled symmetrically by square root of eigenvalues (Oksanen et al., 2018). The proportion of variability in the chemical composition of SOM attributed to each of the RDA axes is shown within parentheses. The colour gradient depicts leaf $\delta^{15}\text{N}$ concentrations; the darker, the higher. RDA revealed a significant association between the chemical composition and $\delta^{15}\text{N}$ for both the pyrolysis and NMR-products in both the L- and F/H-horizons (also see Table S3, S4). The pyrolysis products are carbohydrate, guaiacyl lignin (g-lignin), N compounds (N comp.), phenolic compounds (phenol), syringyl lignin (s-lignin), other aromatic derivatives (aromatic deriv.), aliphatic derivatives (aliphatic deriv.; fatty acid, ketone, alkane and alkene) and others (steroid, vitamin, chlorophyll and hopanoid).

both methods of pyrolysis GC/MS and ^{13}C NMR in both horizons (Table S3). Species loading given from this subset of data demonstrated a similar pattern to that from the complete dataset presented above, primarily separated by g-lignin and carbohydrate for the pyrolysates and by aromatic and O-alkyl C for the NMR-products, respectively (Table S4).

3.4. Lignin and carbohydrate

Lignin:carbohydrate ratios in the pyrolysates increased with $\delta^{15}\text{N}$ in *V. vitis-idaea* leaves (a proxy for N loading) for both soil horizons (Leaf $\delta^{15}\text{N}$: $F_{1, 54} = 38.93, P < 0.001$), with the ratios consistently higher in the L horizon than the F/H (Horizon: $F_{1, 54} = 39.46, P < 0.001$). There was no evidence of interactive effects between leaf $\delta^{15}\text{N}$ and horizon (Leaf $\delta^{15}\text{N}$:Horizon: $F_{1, 54} = 0.20, P > 0.1$, Figs. 5, S9). Consistent results were obtained when a subset of data derived only from the fertilised plot (including the inside, edge and outside) was analysed (Table S5). Person's correlation tests demonstrated that the inverse of lignin:carbohydrate ratios (i.e., carbohydrate:lignin ratios) was significantly correlated with total C mass (kg m^{-2}) in the L-horizon ($P < 0.05, df = 54, r = -0.33$) and in the F/H-horizon ($P < 0.01, df = 54, r = -0.35$), respectively, indicating significant positive associations between lignin:carbohydrate ratios and C mass. G/S-lignin ratios in the pyrolysates tended to increase with $\delta^{15}\text{N}$ in *V. vitis-idaea* leaves (Fig. S10), although it was not significant (Leaf $\delta^{15}\text{N}$: $F_{1, 54} = 3.38, P = 0.072$), with the ratios substantially lower in the L horizon than the F/H (Horizon: $F_{1, 54} = 328.66, P < 0.001$).

4. Discussion

The current study investigated the effects of added N on the variation in chemical composition of SOM in a mature, boreal forest. The results of both the spectrometric and spectroscopic analyses of pyrolysis GC/MS and ^{13}C NMR indicated that N enrichment increased the abundance of lignin-derived compounds at the expense of carbohydrate-derived compounds in both of the L- and F/H-horizons. When analysing data obtained only from the sampling plots at the inside, edge and outside of fertilised plot excluding those from the control plot, there was still a

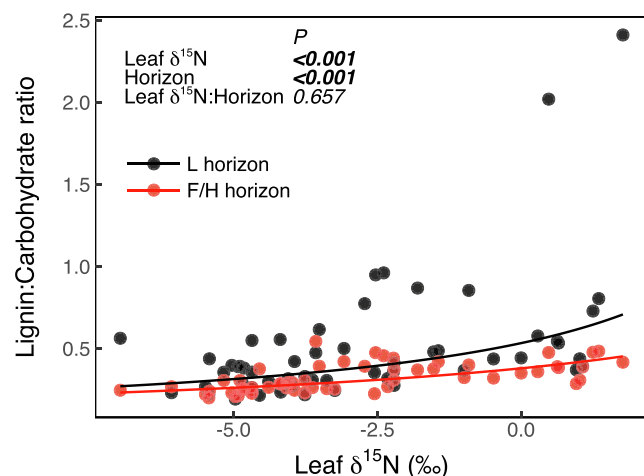


Fig. 5. Relationship between lignin:carbohydrate ratios of pyrolysis products and leaf $\delta^{15}\text{N}$ of *Vaccinium vitis-idaea*. The L- and F/H -horizons are depicted by black and red colours, respectively. The summary of the analysis with linear-mixed effects model is also shown for each tested variable: leaf $\delta^{15}\text{N}$, horizon and their interaction, with significant P values ($P < 0.05$) shown in bold. The response variable (lignin:carbohydrate ratios) was inverse-transformed prior to the analysis. The predicted values were obtained from the model and reverse-transformed, depicted by solid lines (also see Fig S9 for the inverse-transformed ratios). (For interpretation of the references to colour in this figure legend, the reader is referred to the web version of this article.)

significant association between the chemical composition and leaf $\delta^{15}\text{N}$ for both methods of pyrolysis GC/MS and ^{13}C NMR in both horizons (Table S3) as well as a positive relationship between lignin:carbohydrate ratios and leaf $\delta^{15}\text{N}$ (Table S5). Thus, the observed shift in SOM chemical composition was not due to different sampling locations between the control and fertilised plots but likely due to variations in soil N conditions.

In this study, $\delta^{15}\text{N}$ in *V. vitis-idaea* leaves was utilised as a proxy of sampling plot-level long-term N loading. Using isotopically labelled

fertilizer with ^{15}N is a well-established method to trace nutrient uptake by plants (e.g., Jayasundara et al., 2007; Melin et al., 1983; Sebilo et al., 2013), and ^{15}N concentrations in plant tissues depend on application rates of the labelled fertilizer (Adesemoye et al., 2010; Sikora and Enkiri, 2001). The fertilizer used in the currently study was not extraneously labelled but intrinsically enriched in ^{15}N relative to that of the natural abundance in the soil and thus traceable in the dominant shrub species of *V. vitis-idaea* (Fig. 1b). This allowed us to capture the fine-scale spatial variation in fertilizer-N between the soil sampling plots, enabling the investigation into a shift of chemical composition in SOM along the gradient of exogenous N addition. The use of environmental gradients has been a constructive approach to disentangle a complex ecosystem processes (Fernandez and Kennedy, 2016; McGill et al., 2006). Our study demonstrates a gradual change in chemical composition of SOM towards one direction—increased lignin:carbohydrate ratios—with the fertilizer-N gradient, suggesting that N-dependent processes were responsible for the altered properties of SOM under N enrichment in this system.

Our findings of increased lignin:carbohydrate ratios (or an increased fraction of aromatic C at the expense of O-alkyl C in ^{13}C NMR product) are generally consistent with results from studies conducted in temperate hardwood forests with variable rates (30–150 kg N ha^{-1} year $^{-1}$) and duration (6–20 years) of N addition (e.g., Frey et al., 2014; van den Enden et al., 2018), although contrasting results were also reported (e.g., Grandy et al., 2008; Pisani et al., 2015; Zak et al., 2017). In a boreal forest, Höglberg et al. (2020) characterised chemical composition of SOM using ^{13}C NMR along a naturally occurring N gradient and reported higher relative abundance of aromatic C at the high N relative to that of the low N conditions, demonstrating a consistent pattern as the findings in our study. Furthermore, a global meta-analysis by Liu et al. (2016) reported that, in forest ecosystems, N addition increased lignin-derived compounds in soils while decreasing cellulose and not altering lignin in decomposed litter, respectively, although no study from boreal forests was included.

Quantitative and qualitative changes in SOM under N-enriched conditions are often ascribed to changes in microbial and enzymatic activity. It is commonly reported that N addition decreases ligninolytic enzyme activity and increases cellulolytic enzymes (e.g., Rinkes et al., 2016). Chen et al. (2018) summarised 40 studies with N addition experiments including one from a boreal forest, reporting that N addition hampered the activity of ligninolytic enzymes and increased that of cellulolytic enzymes. Altered balance of ligninolytic and cellulolytic enzyme activity under N enrichment leads to a compositional shift in associated organic compounds in SOM (e.g., Cusack et al., 2011; Frey et al., 2004; Zak et al., 2019). Studies on the effects of N addition on enzymes are scarce for boreal forests. Nonetheless, increased cellulolytic enzyme activity was found in a black spruce forest situated in central Alaska after 3 year N addition (100–200 kg N ha^{-1} year $^{-1}$; Allison et al., 2008) and in a heath tundra following 5 year NPK fertilizer treatment (96 kg N ha^{-1} year $^{-1}$; Stark et al., 2014). Thus, our findings from a boreal forest that N-induced relative increases in lignin- to carbohydrate-derivatives were consistent with the predictions made based on those general trends of extracellular enzyme responses to N enrichment in previous studies. Soil acidification induced by N enrichment can also lead to quantitative and qualitative changes in SOM via suppressed microbial activity and the formation of organo-mineral C (Ye et al., 2018); however, this likely plays a relatively little role in boreal and some temperate forests as N-induced changes in soil pH are generally minute in those systems including the current study site (Bonner et al., 2019; Forsmark et al., 2020; Patterson et al., 2012; Swathi et al., 2013; Tian and Niu, 2015).

The mechanisms underlying N-induced changes in enzymatic activity and in associated SOM quality and quantity have long been discussed but are still not completely discerned (e.g., Fog, 1988). The recent study by Bonner et al. (2019) demonstrated suppressed white-rot decomposition relative to brown-rot decay under enriched N conditions in Scots

pine (the same site as the current study) and nearby Norway spruce forests. In their study, whilst lignin-oxidative enzyme activity was decreased under added-N conditions, non-enzymatic lignin oxidation was unaltered. Furthermore, in their study, the abundance of transcripts encoding key enzymes in SOM degradation in the Norway spruce forest revealed decreased expression of class II peroxidase (indicator of white-rot activity) but unchanged expression of iron reduction proteins (indicator of brown-rot activity) in basidiomycete fungi present on/in plant roots under enriched N conditions. Thus, the findings of Bonner et al. (2019) from both enzymatic and metagenomic assays were consistent with the long-known observation that N enrichment suppresses oxidative enzyme synthesis (e.g., Fenn and Kent Kirk, 1981; Kirk and Farrell, 1987). Bonner et al., in line with Fog (1988), attributed this N-induced suppression of ligninolytic enzymes to the idea that N enrichment would cause the spontaneous formation of amino-lignin compounds resulting from oxidative coupling and that would interfere with lignin decomposition, lowering net energy gain from white-rot activity and thus rendering white-rot less competitive against brown-rot decomposition. Hampered white-rot activity (that has the potential to fully decompose a lignocellulose complex) relative to brown-rot decay (that cleaves, yet does not decompose, lignin) is consistent with our findings of the shift in lignin:carbohydrate ratios (Filley et al., 2002; Hatakka and Hammel, 2011). On a similar note, Entwistle et al. (2018) revealed that N enrichment decreased ligninolytic- and increased cellulolytic-fungi following 17 years' N addition (30 kg N ha^{-1} year $^{-1}$) in a temperate hardwood forest. Although fungal community composition has yet to be additionally examined, taken together with the above-mentioned findings reported by Bonner et al. (2019) using enzymatic and metagenomic methods on the same and nearby study sites, the observed changes in SOM chemical composition in the current study may be attributed to altered balance between the two phenotypes of saprotrophs.

An alternative or additional explanation for altered ratios of lignin and carbohydrate-derived compounds is that the chemical composition of the plant litter inputs may have been different between the control and N fertilised sites due to 1) altered chemistry in plant tissues, 2) a shift in vegetation community and/or 3) altered balance of above-ground:belowground litter inputs. However, a long-term N addition experiment nearby our study site (<15 km) examined lignin, cellulose and hemicellulose in aboveground fresh plant litters and mosses in a mixed forest of Norway spruce and Scots pine, demonstrating no evidence of modified properties in those studied materials after 17 years of N treatments (12.5 and 50 kg N ha^{-1} year $^{-1}$; Maaroufi et al., 2016). Also, the above-mentioned global meta-analysis by Liu et al. (2016) concluded that N addition slightly decreased both lignin and cellulose in trees to a similar extent. Thus, neither of those studies supports that the altered chemical composition in SOM resulted from modified properties in plant litters before undergoing decomposition. A shift in vegetation community, especially altered balance between vascular and non-vascular (e.g., moss) plants, can potentially influence lignin:carbohydrate ratios in SOM (Kohl et al., 2018). However, this was unlikely the case in the current study as there was no evidence of changes in C mass (kg m^{-2}) of the moss with the N level (data not shown here). We found a weak positive correlation between G/S-lignin and leaf $\delta^{15}\text{N}$ in this study; although this may indicate a slight increase in relative contribution of Scots pine litter with the N level compared to angiosperm species present at the understorey, this correlation was not statistically significant ($P = 0.072$) and unlikely responsible for the observed changes in lignin:carbohydrate ratios. On the other hand, Lim et al. (2015) demonstrated, at the current study site, that annual net primary productivity of fine roots was significantly reduced at the fertilised plot relative to the control (~33%) while that of foliage did not significantly differ between the treatments in 2012. It has been reported that Klason-lignin contents and associated lignin:carbohydrate ratios in needle litters were higher than those in root litters for Scots pine in a mature Scots pine forest stand situated in central Sweden (Berg, 1984; Berg and Ågren, 1984). Thus, the increased lignin:carbohydrate ratios with the N level observed in our

study may in part have been derived from a relative decrease in fine root production under enriched N conditions.

Long-term N enrichment has been reported to increase C accumulation in temperate and boreal forests (e.g., de Vries et al., 2009; Hyvönen et al., 2008; Maaroufi et al., 2015). At our study site, the thickness of the organic horizon was significantly increased by N addition (Bonner et al., 2019). Forsmark et al. (2020) similarly observed the increased C sequestration following N enrichment after 12 years of N addition treatments in a Scots pine forest nearby our study site (<15 km). They attributed this increase primarily to suppressed soil respiration under ranging N addition rates (2–50 kg N ha⁻¹ year⁻¹); at the same site, Maaroufi et al. (2019) reported N-enrichment-induced decreases in microbial biomass and decomposition rates, suggesting a significant role of reduced microbial decomposition in C sequestration. Indeed, soil CO₂ efflux measured using large chambers (diameter = 5 m, height = 1 m) established in the current study site was reduced by 52% at the fertilised plot compared to the control between 2012 and 2014 (Marshall et al. manuscript in preparation). In line with those findings, higher lignin:carbohydrate ratios under higher N conditions were associated with increased soil C mass in our study. This likely led to overall increases in soil C mass from 0.630 ± 0.274 to 0.825 ± 0.209 kg m⁻² in the L horizon and from 0.910 ± 0.337 to 1.268 ± 0.264 kg m⁻² in the F/H horizon from the control to the inside of fertilised plot, respectively (mean ± 95% confidence interval, n = 11 for the control and 15 for the fertilised plot).

Both pyrolysis GC/MS and ¹³C NMR are semi-quantitative techniques and therefore they only provide limited information on actual quantities of different C compounds present in soil (Feng and Simpson, 2011; Kögel-Knabner, 2000; Marques and Pereira, 2013; Saiz-Jimenez, 1994; Tolu et al., 2015). Nevertheless, Nelson and Baldock (2005) developed a molecular mixing model that enabled estimating the relative contribution of lignin and carbohydrate compounds to the total soil organic C pool from the chemical shift regions obtained from ¹³C NMR. We applied this mixing model to the ¹³C NMR-product data obtained in this study and computed area-based C mass of those compounds. Regressing the resulting estimates of C mass against leaf δ¹⁵N, we arrived at an estimate of an exponential rate of change of +1.7% and +6.6% for lignin C in the L and F/H horizons respectively, and -2.5% and +3.5% for carbohydrate C respectively (see Table S6, Fig S11 and the descriptions therein for the details). These estimates correspond to the maximum potential increase in C mass of 0.18 and 0.03 kg m⁻² for lignin and carbohydrate compounds in the organic horizon between the low and high ends of leaf δ¹⁵N observed in the present study (-6.97 to 1.77‰, Fig. 1b), respectively. Taken together with the positive correlation between lignin:carbohydrate ratios and soil C mass, this result suggests that N enrichment suppresses lignin decomposition relative to carbohydrate compounds and selectively preserves lignin-derived compounds. Although absolute quantification of lignin and carbohydrate C mass is still required using methods like wet-chemistry techniques (Feng and Simpson, 2011), it is plausible that a larger fraction of incompletely degraded lignin resulting from a shift from white- to brown-rot activity may have contributed to the increased C mass (Entwistle et al., 2018; Frey et al., 2014).

Our study revealed that the lignin- and carbohydrate-derived compounds were the primary drivers of the compositional shift in SOM (Fig. 4), with relatively small contribution of the other compounds. Nevertheless, the relative abundance of N compounds in the pyrolysates was found to be significantly correlated with leaf δ¹⁵N, indicating that N-enrichment enhanced the contribution of soil organic nitrogen to SOM in our study site. In the L-horizon, the N compound fraction was mainly composed of diketopiperazines (cyclo (Pro-Pro) and cyclo leucine-Pro (Leu-Pro)) and diketodipyrrole (Fig S3). Diketopiperazines are common pyrolysis-products of proteins, peptides and amino acids (Fabbri et al., 2012). These compounds could come from either fungi, bacteria, plants or fauna (Abelenda et al., 2011; Holden et al., 1999; Stankiewicz et al., 1996). For the F/H-horizon, the N compound fraction was mainly

attributed to methyl N-acetyl-α-D-glucosaminide followed by pyrrole/pyridine (Fig. S3). N-acetylglycosamine compounds are generally considered to originate from chitin derived from fungal cell walls or microarthropod exoskeletons and from N-acetylglucosamine present in peptidoglycan in bacterial cell walls (Buurman et al., 2007; Frey et al., 2004; Guggenberger et al., 1999). Hobbie et al. (2019) reported that N addition increased N uptake by ectomycorrhizal fungi in the F horizon in the same study site as ours. Thus, our data suggest that microbial N contributed significantly to soil accumulation of added-N in the F/H-horizon.

Suberin and cutin are composed of long-chain fatty acids, comprising cell walls on the outermost layer of plants (leaves, barks and roots) and coating plant tissues (Kögel-Knabner, 2002). They are relatively more recalcitrant than carbohydrates and likely remain in humus following a course of litter decomposition (Feng and Simpson, 2011; Lorenz et al., 2007). The pyrolysates of these compounds are generally found in aliphatic compound groups like fatty acids, n-alkane and n-alkene (Abelenda et al., 2011 and references therein; de Leeuw and Baas, 1993; González-Vila et al., 1996; Nierop, 1998; Tegelaar et al., 1989). The alkyl C region in ¹³C NMR is generally considered to originate from the fatty acids derived from suberin and cutin (Nierop et al., 1999; Winkler et al., 2005). The relative abundance of aliphatic derivatives in the pyrolysates and that of alkyl C in ¹³C NMR were indeed higher in the F/H-horizon compared to the L-horizon in our study (Figs. 2 and 3). Some studies report that suberin- and cutin-derived compounds in SOM are increased by N addition in temperate forests, contributing to C sequestration (e.g., Feng et al., 2010; Pisani et al., 2015; van den Enden et al., 2018; Wang et al., 2019). In contrast, RDA analysis of the pyrolysates in our study showed little contribution of aliphatic derivatives to the shift in SOM chemical composition with the N level (Fig. 4). Also, there was little evidence of a shift in alkyl C with the N level on the ¹³C NMR products in either the L- or F/H-horizon. Thus, we found no evidence of contribution from suberin- or cutin-derived compounds to the altered SOM chemical composition in the enriched-N soil in our study. It should, however, be noted that suberin- and cutin-derived compounds (or fatty acids) may have been underestimated in our study. The thermal degradation of suberin requires high energy and may not be complete at temperatures below 550 °C in the pyrolyser (Marques and Pereira, 2013). The soil samples were pyrolysed at 450 °C in our study so that suberin may not have been thoroughly degraded and hence underestimated.

Lignin:carbohydrate ratios were found to be higher in the L- than F/H-horizon in our study. This was contrary to our expectation that the ratios would be higher in the more processed horizon of F/H than the L due to selective decomposition of carbohydrate materials. As polysaccharides of cellulose and hemicellulose in fresh litter are hydrolysable and generally less recalcitrant than non-hydrolysable lignin (Eriksson et al., 1990; Hudson, 1968), carbohydrates are expected to be more preferentially decomposed over lignin during an early phase of litter decomposition (Berg and Matzner, 1997; McTiernan et al., 2003). However, this does not appear to be the case in the current study. It may be in part because the origin of litter inputs to the L-horizon had higher lignin:carbohydrate ratios than that for the F/H horizon. The primary litter inputs to the upper layer of the organic horizon likely originate from aboveground parts of plants like pine needles, twigs and branches and some roots from vegetation at the forest floor (e.g., *V. vitis-idaea*), whereas the litter inputs to the deeper layer are likely derived from tree roots and root-associated mycorrhizae (Neville et al., 2002; Persson, 1983); as mentioned above Klason-lignin contents were reported to be higher in needles than in root litters for Scots pine (Berg, 1984; Berg and Ågren, 1984). Also, roots of *V. vitis-idaea* were reported to have much higher lignin contents and lignin:carbohydrate ratios compared to those of Scots pine (Berg, 1984), likely being more abundant in the upper layer of the organic horizon in a mature Scots pine forest (Persson, 1983)—which was also indicated by significantly lower G/S-lignin ratios in the L horizon than F/H in our study. Thus, the inputs from needle and *V. vitis-*

idaea root litters might have been contributed to the higher lignin:carbohydrate ratios in the L horizon compared to the F/H horizon.

There are also a couple of potential, additional explanations for higher lignin:carbohydrate ratios in the L- than F/H-horizon. First, the balance of cellulose and lignin decomposition could substantially vary due to environmental factors such as temperature and moisture (e.g., Donnelly et al., 1990; Wickland and Neff, 2008). Second, some white-rot fungi are reported to selectively decompose lignin and leave cellulose and/or hemicellulose behind (e.g., Enoki et al., 1988; Hakala et al., 2004; Otjen and Blanchette, 1985). Third, lignin decomposition may have actually occurred at a faster rate than that for carbohydrates as outlined in Klotzbücher et al. (2011) postulating a new lignin decomposition framework that a lignin fraction can be decomposed rapidly where there is sufficient amount of bioavailable C that facilitates the synthesis of lignin decomposing enzymes. Last, the carbohydrates in the F/H-horizon in part may also have originated in microbes (e.g., furans and furanones, Fig S1; Buurman and Roscoe, 2011). Thus, the higher lignin:carbohydrate ratios in the L- relative to F/H-horizon observed in our study may have been due to qualitative difference in input litters, selective delignification of plant litter and/or microbial contribution.

5. Conclusion

Our study aimed to assess the SOM responses to N addition in a boreal forest using pyrolysis GC/MS and ^{13}C NMR and, as such, it would provide novel insights into soil C and N dynamics in the high latitude ecosystems. Decadal N addition treatment led to a compositional shift of SOM in the organic horizon, with increased lignin-derived compounds relative to carbohydrate-derived, accompanied by an increase in soil C mass (kg m^{-2}). Our findings corroborate the hypothesis that N-enrichment suppresses enzymatic white-rot lignin mineralisation relative to non-enzymatic brown-rot lignin oxidation (Bonner et al., 2019). Long-term N addition thus altered both the quality and quantity of SOM, with potential ramifications on the capacity of forest ecosystems to sequester C and hence on the role of forests in mitigating increased CO_2 emissions.

Declaration of Competing Interest

The authors declare that they have no known competing financial interests or personal relationships that could have appeared to influence the work reported in this paper.

Acknowledgements

This work was supported by Knut and Alice Wallenberg Foundation (Knut och Alice Wallenbergs Stiftelse) [grant number 2015.0047] and the Kempe Foundations (Kempestiftelsen). Also, we acknowledge the Swedish NMR centre at Umeå University, Knut and Alice Wallenberg foundation program “NMR for Life” and SciLifeLab for NMR support. Furthermore, we thank Jenny Ekman and Junko Takahashi Schmidt for sample analysis, Julie Tolu for the advice on analysing pyrolysis data and Jolanda Snellenberg and Tommy Andersson for assisting fieldwork. Mark Bonner provided invaluable assistance with data analysis and interpretation.

Data accessibility

The raw data and the R scripts that reproduce the results presented in this paper are available to download from Zenodo: <https://doi.org/10.5281/zenodo.4419546>.

Appendix A. Supplementary data

Supplementary data to this article can be found online at <https://doi.org/10.1016/j.geoderma.2020.114906>.

References

- Abelenda, M.S., Buurman, P., Arbestain, M.C., Kaal, J., Martinez-Cortizas, A., Gartzia-Bengoetxea, N., Macías, F., 2011. Comparing NaOH-extractable organic matter of acid forest soils that differ in their pedogenic trends: a pyrolysis-GC/MS study. Eur. J. Soil Sci. 62, 834–848. <https://doi.org/10.1111/j.1365-2389.2011.01404.x>
- Adesemoye, A.O., Torbert, H.A., Klopper, J.W., 2010. Increased plant uptake of nitrogen from ^{15}N -depleted fertilizer using plant growth-promoting rhizobacteria. Appl. Soil Ecol. 46 (1), 54–58. <https://doi.org/10.1016/j.apsoil.2010.06.010>
- Allison, S.D., Czimczik, C.I., Treseder, K.K., 2008. Microbial activity and soil respiration under nitrogen addition in Alaskan boreal forest. Glob. Change Biol. 14, 1156–1168. <https://doi.org/10.1111/j.1365-2486.2008.01549.x>
- Bates, D., Mächler, M., Bolker, B., Walker, S., 2015. Fitting Linear Mixed-Effects Models Using lme4. J. Stat. Softw. 67, 1–48. <https://doi.org/10.18637/jss.v067.i01>
- Batjes, N.H., 1996. Total carbon and nitrogen in the soils of the world. Eur. J. Soil Sci. 47 (2), 151–163. <https://doi.org/10.1111/j.1365-2389.1996.tb01386.x>
- Berg, B., 1984. Decomposition of root litter and some factors regulating the process: Long-term root litter decomposition in a scots pine forest. Soil Biol. Biochem. 16 (6), 609–617. [https://doi.org/10.1016/0038-0717\(84\)90081-6](https://doi.org/10.1016/0038-0717(84)90081-6)
- Berg, B., Ågren, G.I., 1984. Decomposition of needle litter and its organic chemical components: theory and field experiments. Long-term decomposition in a Scots pine forest. III. Canadian J. Botany 62 (12), 2880–2888. <https://doi.org/10.1139/b84-384>
- Berg, B., Matzner, E., 1997. Effect of N deposition on decomposition of plant litter and soil organic matter in forest systems. Environ. Rev. 5 (1), 1–25. <https://doi.org/10.1139/a96-017>
- Bonner, M.T.L., Castro, D., Schneider, A.N., Sundström, G., Hurry, V., Street, N.R., Näsholm, T., 2019. Why does nitrogen addition to forest soils inhibit decomposition? Soil Biol. Biochem. 137, 107570. <https://doi.org/10.1016/j.soilbio.2019.107570>
- Buurman, P., Nierop, K.G.J., Kaal, J., Senesi, N., 2009. Analytical pyrolysis and thermally assisted hydrolysis and methylation of EUROSOL humic acid samples — A key to their source. Geoderma 150 (1-2), 10–22. <https://doi.org/10.1016/j.geoderma.2008.12.012>
- Buurman, P., Roscoe, R., 2011. Different chemical composition of free light, occluded light and extractable SOM fractions in soils of Cerrado and tilled and untilled fields, Minas Gerais, Brazil: a pyrolysis-GC/MS study. Eur. J. Soil Sci. 62, 253–266. <https://doi.org/10.1111/j.1365-2389.2010.01327.x>
- Buurman, P., Schellekens, J., Fritze, H., Nierop, K.G.J., 2007. Selective depletion of organic matter in mottled podzol horizons. Soil Biol. Biochem. 39 (2), 607–621. <https://doi.org/10.1016/j.soilbio.2006.09.012>
- Chen, J.I., Luo, Y., van Groenigen, K.J., Hungate, B.A., Cao, J., Zhou, X., Wang, R.-W., 2018. A keystone microbial enzyme for nitrogen control of soil carbon storage. Sci. Adv. 4 (8), eaq1689. <https://doi.org/10.1126/sciadv.aq1689>
- Chen, Y., Chen, J.I., Luo, Y., 2019. Data-driven ENZYME (DENZY) model represents soil organic carbon dynamics in forests impacted by nitrogen deposition. Soil Biol. Biochem. 138, 107575. <https://doi.org/10.1016/j.soilbio.2019.107575>
- Clemmensen, K.E., Bahr, A., Ovaskainen, O., Dahlberg, A., Ekblad, A., Wallander, H., Stenlid, J., Finlay, R.D., Wardle, D.A., Lindahl, B.D., 2013. Roots and associated fungi drive long-term carbon sequestration in boreal forest. Science 339 (6127), 1615–1618. <https://doi.org/10.1126/science.1231923>
- Crawley, M.J., 2012. The R Book, second ed. John Wiley & Sons Ltd, West Sussex, UK.
- Cusack, D.F., Silver, W.L., Torn, M.S., Burton, S.D., Firestone, M.K., 2011. Changes in microbial community characteristics and soil organic matter with nitrogen additions in two tropical forests. Ecology 92 (3), 621–632. <https://doi.org/10.1890/10-0459.1>
- Davidson, E.A., 2009. The contribution of manure and fertilizer nitrogen to atmospheric nitrous oxide since 1860. Nat. Geosci. 2 (9), 659–662. <https://doi.org/10.1038/ngeo608>
- de Leeuw, J.W., Baas, M., 1993. The behaviour of esters in the presence of tetramethylammonium salts at elevated temperatures; flash pyrolysis or flash chemolysis? J. Anal. Appl. Pyrol. 26 (3), 175–184. [https://doi.org/10.1016/0162-2370\(93\)80065-8](https://doi.org/10.1016/0162-2370(93)80065-8)
- de Vries, W., Solberg, S., Dobbertin, M., Sterba, H., Laubhann, D., van Oijen, M., Evans, C., Gundersen, P., Kros, J., Wamelink, G.W.W., Reinds, G.J., Sutton, M.A., 2009. The impact of nitrogen deposition on carbon sequestration by European forests and heathlands. Forest Ecology and Management, The relative importance of nitrogen deposition and climate change on the sequestration of carbon by forests in Europe. 258 (8), 1814–1823. <https://doi.org/10.1016/j.foreco.2009.02.034>
- Deluca, T.H., Boisvenue, C., 2012. Boreal forest soil carbon: distribution, function and modelling. Forestry: Int. J. Forest Res. 85 (2), 161–184. <https://doi.org/10.1093/forestry/cps003>
- Dignac, M., Kogel-Knabner, I., Michel, K., Matzner, E., Knicker, H., 2002. Chemistry of soil organic matter as related to C: N in Norway spruce forest (*Picea abies* (L.) Karst.) floors and mineral soils. J. Plant Nutrition Soil Sci. 165, 281–289. [https://doi.org/10.1002/1522-2624\(200206\)165:3<281::aid-jpln281>3.0.co;2-a](https://doi.org/10.1002/1522-2624(200206)165:3<281::aid-jpln281>3.0.co;2-a)
- Donnelly, P.K., Entry, J.A., Crawford, D.L., Cromack, K., 1990. Cellulose and lignin degradation in forest soils: Response to moisture, temperature, and acidity. Microb. Ecol. 20 (1), 289–295. <https://doi.org/10.1007/BF02543884>
- Enoki, A., Tanaka, H., Fuse, G., 1988. Degradation of lignin-related compounds, pure cellulose, and wood components by white-rot and brown-rot fungi. Holzforschung 42 (2), 85–93. <https://doi.org/10.1515/hfsg.1988.42.2.85>
- Entwistle, E.M., Zak, D.R., Argiroff, W.A., 2018. Anthropogenic N deposition increases soil C storage by reducing the relative abundance of lignolytic fungi. Ecol. Monogr. 88 (2), 225–244. <https://doi.org/10.1002/ecm.1288>

- Eriksson, K.-E.L., Blanchette, R.A., Ander, P., 1990. Microbial and Enzymatic Degradation of Wood and Wood Components, Springer Series in Wood Science. Springer Berlin Heidelberg, Berlin, Heidelberg. doi:10.1007/978-3-642-46687-8.
- Fabbri, D., Adamiano, A., Falini, G., De Marco, R., Mancini, I., 2012. Analytical pyrolysis of dipeptides containing proline and amino acids with polar side chains. Novel 2,5-diketopiperazine markers in the pyrolysates of proteins. *J. Anal. Appl. Pyrol.* 95, 145–155. <https://doi.org/10.1016/j.jaat.2012.02.001>.
- Feng, X., Simpson, A.J., Schlesinger, W.H., Simpson, M.J., 2010. Altered microbial community structure and organic matter composition under elevated CO₂ and N fertilization in the duke forest. *Glob. Change Biol.* 16, 2104–2116. <https://doi.org/10.1111/j.1365-2486.2009.02080.x>.
- Feng, X., Simpson, M.J., 2011. Molecular-level methods for monitoring soil organic matter responses to global climate change. *J. Environ. Monit.* 13, 1246–1254. <https://doi.org/10.1039/C0EM00752H>.
- Fenn, P., Kent Kirk, T., 1981. Relationship of nitrogen to the onset and suppression of ligninolytic activity and secondary metabolism in *Phanerochaete chrysosporium*. *Arch. Microbiol.* 130 (1), 59–65. <https://doi.org/10.1007/BF00527073>.
- Fernandez, C.W., Kennedy, P.G., 2016. Revisiting the ‘Gadgil effect’: do interguild fungal interactions control carbon cycling in forest soils? *New Phytol.* 209 (4), 1382–1394. <https://doi.org/10.1111/nph.13648>.
- Filley, T.R., Cody, G.D., Goodell, B., Jellison, J., Noser, C., Ostrofsky, A., 2002. Lignin demethylation and polysaccharide decomposition in spruce sapwood degraded by brown rot fungi. *Org Geochem.* 33 (2), 111–124. [https://doi.org/10.1016/S0146-6380\(01\)00144-9](https://doi.org/10.1016/S0146-6380(01)00144-9).
- Fox, K., 1988. The effect of added nitrogen on the rate of decomposition of organic matter. *Biol. Rev.* 63 (3), 433–462. <https://doi.org/10.1111/bvr.1988.63.issue-310.1111/j.1469-185X.1988.tb00725.x>.
- Forsmark, B., Nordin, A., Maaroufi, N.I., Lundmark, T., Gundale, M.J., 2020. Low and high nitrogen deposition rates in northern coniferous forests have different impacts on aboveground litter production, soil respiration, and soil carbon stocks. *Ecosystems* 23 (7), 1423–1436. <https://doi.org/10.1007/s10021-020-00478-8>.
- Fox, J., Weisberg, S., 2011. An R companion to applied regression, second ed. SAGE Publications Inc, Thousand Oaks, CA.
- Frey, S.D., Knorr, M., Parrent, J.L., Simpson, R.T., 2004. Chronic nitrogen enrichment affects the structure and function of the soil microbial community in temperate hardwood and pine forests. Forest Ecology and Management, The Harvard Forest (USA) Nitrogen Saturation Experiment: Results from the First 15 Years 196, 159–171. doi:10.1016/j.foreco.2004.03.018.
- Frey, S.D., Ollinger, S., Nadelhoffer, K., Bowden, R., Brzostek, E., Burton, A., Caldwell, B. A., Crow, S., Goodale, C.L., Grandy, A.S., Finzi, A., Kramer, M.G., Lajtha, K., LeMoine, J., Martin, M., McDowell, W.H., Minocha, R., Sadowsky, J.J., Tempier, P. H., Wickings, K., 2014. Chronic nitrogen additions suppress decomposition and sequester soil carbon in temperate forests. *Biogeochemistry* 121 (2), 305–316. <https://doi.org/10.1007/s10533-014-0004-0>.
- Fung, B.M., Khitrin, A.K., Ermolaev, K., 2000. An improved broadband decoupling sequence for liquid crystals and solids. *J. Magn. Reson.* 142 (1), 97–101. <https://doi.org/10.1006/jmre.1999.1896>.
- Galloway, J.N., Townsend, A.R., Erisman, J.W., Bekunda, M., Cai, Z., Freney, J.R., Martínez, L.A., Seitzinger, S.P., Sutton, M.A., 2008. Transformation of the nitrogen cycle: recent trends, questions, and potential solutions. *Science* 320 (5878), 889–892. <https://doi.org/10.1126/science.1136674>.
- Gerber, L., Eliasson, M., Trygg, J., Moritz, T., Sundberg, B., 2012. Multivariate curve resolution provides a high-throughput data processing pipeline for pyrolysis-gas chromatography/mass spectrometry. *J. Anal. Appl. Pyrol.* 95, 95–100. <https://doi.org/10.1016/j.jaat.2012.01.011>.
- González-Vila, F.J., Del Rio, J.C., Martin, F., Verdejo, T., 1996. Pyrolytic alkylation-gas chromatography-mass spectrometry of model polymers Further insights into the mechanism and scope of the technique. *J. Chromatography A*, 4th International Symposium on Hyphenated Techniques in Chromatography and Hyphenated Chromatographic Analyzers 750 (1-2), 155–160. [https://doi.org/10.1016/0021-9673\(96\)00539-0](https://doi.org/10.1016/0021-9673(96)00539-0).
- Goodell, B., Jellison, J., Liu, J., Daniel, G., Paszczynski, A., Fekete, F., Krishnamurthy, S., Jun, L., Xu, G., 1997. Low molecular weight chelators and phenolic compounds isolated from wood decay fungi and their role in the fungal biodegradation of wood. *J. Biotech.*, Low Molecular Weight Compounds Lignin Degradation 53, 133–162. [https://doi.org/10.1016/S0168-1656\(97\)01681-7](https://doi.org/10.1016/S0168-1656(97)01681-7).
- Grandy, A.S., Sinsabaugh, R.L., Neff, J.C., Stursova, M., Zak, D.R., 2008. Nitrogen deposition effects on soil organic matter chemistry are linked to variation in enzymes, ecosystems and size fractions. *Biogeochemistry* 91 (1), 37–49. <https://doi.org/10.1007/s10533-008-9257-9>.
- Guggenberger, G., Frey, S.D., Six, J., Paustian, K., Elliott, E.T., 1999. Bacterial and fungal cell-wall residues in conventional and no-tillage agroecosystems. *Soil Sci. Soc. Am. J.* 63 (5), 1188–1198. <https://doi.org/10.2136/sssaj1999.6351188x>.
- Guggenberger, G., Zech, W., Schulten, H.-R., 1994. Formation and mobilization pathways of dissolved organic matter: evidence from chemical structural studies of organic matter fractions in acid forest floor solutions. *Org Geochem.* 21 (1), 51–66. [https://doi.org/10.1016/0146-6380\(94\)90087-6](https://doi.org/10.1016/0146-6380(94)90087-6).
- Hakala, T.K., Maijala, P., Konn, J., Hatakka, A., 2004. Evaluation of novel wood-rotting polypores and corticioid fungi for the decay and biopulping of Norway spruce (*Picea abies*) wood. *Enzyme Microb. Technol.* 34 (3-4), 255–263. <https://doi.org/10.1016/j.enzmictec.2003.10.014>.
- Harrysson Drotz, S., Sparman, T., Schleucher, J., Nilsson, M., Öquist, M.G., 2010. Effects of soil organic matter composition on unfrozen water content and heterotrophic CO₂ production of frozen soils. *Geochim. Cosmochim. Acta* 74 (8), 2281–2290. <https://doi.org/10.1016/j.gca.2010.01.026>.
- Hasselquist, N.J., Metcalfe, D.B., Höglberg, P., 2012. Contrasting effects of low and high nitrogen additions on soil CO₂ flux components and ectomycorrhizal fungal sporocarp production in a boreal forest. *Glob. Change Biol.* 18 (12), 3596–3605. <https://doi.org/10.1111/gcb.12001>.
- Hatakka, A., Hammel, K.E., 2011. Fungal Biodegradation of Lignocelluloses. In: Hofrichter, M. (Ed.), Industrial Applications. Springer, Berlin Heidelberg, Berlin, Heidelberg, pp. 319–340. https://doi.org/10.1007/978-3-642-11458-8_15.
- Hättenschwiler, S., Tiunov, A.V., Scheu, S., 2005. Biodiversity and litter decomposition in terrestrial ecosystems. *Annual Review of Ecology, Evolution, and Systematics* 36 (1), 191–218. <https://doi.org/10.1146/annurev.ecolsys.36.112904.151932>.
- Hobbie, E.A., Chen, J., Hasselquist, N.J., 2019. Fertilization alters nitrogen isotopes and concentrations in ectomycorrhizal fungi and soil in pine forests. *Fungal Ecology* 39, 267–275. <https://doi.org/10.1016/j.funeco.2018.12.013>.
- Höglberg, M.N., Skjellberg, U., Höglberg, P., Knicker, H., 2020. Does ectomycorrhiza have a universal key role in the formation of soil organic matter in boreal forests? *Soil Biol. Biochem.* 140, 107635. <https://doi.org/10.1016/j.soilbio.2019.107635>.
- Holden, M.T.G., Ram Chhabra, S., De Nys, R., Stead, P., Bainton, N.J., Hill, P.J., Manefield, M., Kumar, N., Labatte, M., England, D., Rice, S., Givskov, M., Salmond, G.P.C., Stewart, G.S.A.B., Bycroft, B.W., Kjelleberg, S., Williams, P., 1999. Quorum-sensing cross talk: isolation and chemical characterization of cyclic dipeptides from *Pseudomonas aeruginosa* and other Gram-negative bacteria. *Mol. Microbiol.* 33 (6), 1254–1266. <https://doi.org/10.1046/j.1365-2958.1999.01577.x>.
- Hudson, H.J., 1968. The ecology of fungi on plant remains above the soil. *New Phytol.* 67 (4), 837–874. <https://doi.org/10.1111/nph.1968.67.issue-410.1111/j.1469-8137.1968.tb06399.x>.
- Hyvönen, R., Persson, T., Andersson, S., Olsson, B., Ågren, G.I., Linder, S., 2008. Impact of long-term nitrogen addition on carbon stocks in trees and soils in northern Europe. *Biogeochemistry* 89 (1), 121–137. <https://doi.org/10.1007/s10533-007-9121-3>.
- IPCC, 2013. Climate Change 2013: The Physical Science Basis. Contribution of Working Group I to the Fifth Assessment Report of the Intergovernmental Panel on Climate Change. Cambridge University Press, Cambridge, United Kingdom and New York, NY, USA.
- Janssens, I.A., Dieleman, W., Luyssaert, S., Subke, J.-A., Reichstein, M., Ceulemans, R., Ciais, P., Dolman, A.J., Grace, J., Matteucci, G., Papale, D., Piao, S.L., Schulze, E.-D., Tang, J., Law, B.E., 2010. Reduction of forest soil respiration in response to nitrogen deposition. *Nat. Geosci.* 3 (5), 315–322. <https://doi.org/10.1038/ngeo844>.
- Jayasundara, S., Wagner-Riddle, C., Parkin, G., von Bertoldi, P., Warland, J., Kay, B., Voroney, P., 2007. Minimizing nitrogen losses from a corn-soybean-winter wheat rotation with best management practices. *Nutr. Cycl. Agroecosyst.* 79 (2), 141–159. <https://doi.org/10.1007/s10705-007-9103-9>.
- Jonsson, P., Johansson, A.I., Gullberg, J., Trygg, J., A, J., Grung, B., Marklund, S., Sjöström, M., Antti, H., Moritz, T., 2005. High-throughput data analysis for detecting and identifying differences between samples in GC/MS-based metabolomic analyses. *Anal. Chem.* 77 (17), 5635–5642. [https://doi.org/10.1021/ac050601e.10.1021/ac050601e.s001](https://doi.org/10.1021/ac050601e.10.1021/ac050601e.10.1021/ac050601e.s001).
- Kenward, M.G., Roger, J.H., 1997. Small sample inference for fixed effects from restricted maximum likelihood. *Biometrics* 53, 983–997. <https://doi.org/10.2307/2533558>.
- Kirk, T.K., Farrell, R.L., 1987. Enzymatic “Combustion”: The Microbial Degradation of Lignin. *Annu. Rev. Microbiol.* 41 (1), 465–501. <https://doi.org/10.1146/annurev.mi.41.100187.002341>.
- Kirschbaum, M.U.F., 2000. Will changes in soil organic carbon act as a positive or negative feedback on global warming? *Biogeochemistry* 48, 21–51. <https://doi.org/10.1023/A:1006238902976>.
- Klotzbücher, T., Kaiser, K., Guggenberger, G., Gatzek, C., Kalbitz, K., 2011. A new conceptual model for the fate of lignin in decomposing plant litter. *Ecology* 92 (5), 1052–1062. <https://doi.org/10.1890/10-1307.1>.
- Kögel-Knabner, I., 2002. The macromolecular organic composition of plant and microbial residues as inputs to soil organic matter. *Soil Biol. Biochem.* 34, 139–162. [https://doi.org/10.1016/S0038-0717\(01\)00158-4](https://doi.org/10.1016/S0038-0717(01)00158-4).
- Kögel-Knabner, I., 2000. Analytical approaches for characterizing soil organic matter. *Org. Geochem.* 31 (7-8), 609–625. [https://doi.org/10.1016/S0146-6380\(00\)00042-5](https://doi.org/10.1016/S0146-6380(00)00042-5).
- Kohl, L., Philben, M., Edwards, K.A., Podrebarac, F.A., Warren, J., Ziegler, S.E., 2018. The origin of soil organic matter controls its composition and bioreactivity across a mesic boreal forest latitudinal gradient. *Glob. Change Biol.* 24 (2), e458–e473. <https://doi.org/10.1111/gcb.2018.24.issue-210.1111/gcb.13887>.
- Kuznetsova, A., Brockhoff, P.B., Christensen, R.H.B., 2017. lmerTest Package: Tests in Linear Mixed Effects Models. *J. Stat. Softw.* 82, 1–26. <https://doi.org/10.18637/jss.v082.i13>.
- Lal, R., 2005. Forest soils and carbon sequestration. *Forest Ecology and Management*, Forest Soils Research: Theory, Reality and its Role in Technology 220, 242–258. doi: 10.1016/j.foreco.2005.08.015.
- Legendre, L., Legendre, P., 2012. Numerical ecology. Elsevier, Amsterdam.
- Lenardon, M.D., Munro, C.A., Gow, N.A.R., 2010. Chitin synthesis and fungal pathogenesis. *Current Opinion in Microbiology*, Host-Microbe Interactions: Fungi/Parasites/Viruses 13 (4), 416–423. <https://doi.org/10.1016/j.mib.2010.05.002>.
- Lim, H., Oren, R., Palmroth, S., Tor-ngern, P., Mörling, T., Näsholm, T., Lundmark, T., Helmsaari, H.-S., Leppälämmi-Kujansuu, J., Linder, S., 2015. Inter-annual variability of precipitation constrains the production response of boreal *Pinus sylvestris* to nitrogen fertilization. *For. Ecol. Manage.* 348, 31–45. <https://doi.org/10.1016/j.foreco.2015.03.029>.
- Liu, J., Wu, N., Wang, H., Sun, J., Peng, B.o., Jiang, P., Bai, E., 2016. Nitrogen addition affects chemical compositions of plant tissues, litter and soil organic matter. *Ecology* 97 (7), 1796–1806. <https://doi.org/10.1890/15-1683.1>.

- Liu, L., Greaver, T.L., 2010. A global perspective on belowground carbon dynamics under nitrogen enrichment. *Ecol. Lett.* 13, 819–828. <https://doi.org/10.1111/j.1461-0248.2010.01482.x>.
- Lorenz, K., Lal, R., Preston, C.M., Nierop, K.G.J., 2007. Strengthening the soil organic carbon pool by increasing contributions from recalcitrant aliphatic bio(macro)molecules. *Geoderma* 142 (1-2), 1–10. <https://doi.org/10.1016/j.geoderma.2007.07.013>.
- Maaroufi, N.I., Nordin, A., Hasselquist, N.J., Bach, L.H., Palmqvist, K., Gundale, M.J., 2015. Anthropogenic nitrogen deposition enhances carbon sequestration in boreal soils. *Glob. Change Biol.* 21 (8), 3169–3180. <https://doi.org/10.1111/gcb.12904>.
- Maaroufi, N.I., Nordin, A., Palmqvist, K., Gundale, M.J., Bassirirad, H., 2016. Chronic nitrogen deposition has a minor effect on the quantity and quality of aboveground litter in a boreal forest. *PLoS ONE* 11 (8), e0162086. <https://doi.org/10.1371/journal.pone.0162086>.
- Maaroufi, N.I., Nordin, A., Palmqvist, K., Hasselquist, N.J., Forsmark, B., Rosenstock, N.P., Wallander, H., Gundale, M.J., 2019. Anthropogenic nitrogen enrichment enhances soil carbon accumulation by impacting saprotrophs rather than ectomycorrhizal fungal activity. *Glob. Change Biol.* 25 (9), 2900–2914. <https://doi.org/10.1111/gcb.14722>.
- Malhi, Y., Baldocci, D.D., Jarvis, P.G., 1999. The carbon balance of tropical, temperate and boreal forests. *Plant, Cell Environ.* 22 (6), 715–740. <https://doi.org/10.1046/j.1365-3040.1999.00453.x>.
- Marques, A.V., Pereira, H., 2013. Lignin monomeric composition of corks from the barks of *Betula pendula*, *Quercus suber* and *Quercus cerris* determined by Py-GC-MS/FID. *J. Anal. Appl. Pyrol.* 100, 88–94. <https://doi.org/10.1016/j.jaap.2012.12.001>.
- McGill, B., Enquist, B., Weiher, E., Westoby, M., 2006. Rebuilding community ecology from functional traits. *Trends Ecol. Evol.* 21 (4), 178–185. <https://doi.org/10.1016/j.tree.2006.02.002>.
- McTiernan, K.B., Coûteaux, M.-M., Berg, B., Berg, M.P., Calvo de Anta, R., Gallardo, A., Kratz, W., Piussi, P., Remacle, J., Virzo De Santo, A., 2003. Changes in chemical composition of *Pinus sylvestris* needle litter during decomposition along a European coniferous forest climatic transect. *Soil Biol. Biochem.* 35 (6), 801–812. [https://doi.org/10.1016/S0038-0717\(03\)00107-X](https://doi.org/10.1016/S0038-0717(03)00107-X).
- Melin, J., Nömmik, H., Lohm, U., Flower-Ellis, J., 1983. Fertilizer nitrogen budget in a Scots pine ecosystem attained by using root-isolated plots and ^{15}N tracer technique. *Plant Soil* 74 (2), 249–263. <https://doi.org/10.1007/BF02143615>.
- Morcombe, C.R., Zilm, K.W., 2003. Chemical shift referencing in MAS solid state NMR. *J. Magn. Reson.* 162 (2), 479–486. [https://doi.org/10.1016/S1090-7807\(03\)00082-X](https://doi.org/10.1016/S1090-7807(03)00082-X).
- Nelson, P.N., Baldock, J.A., 2005. Estimating the molecular composition of a diverse range of natural organic materials from solid-state ^{13}C NMR and elemental analyses. *Biogeochemistry* 72 (1), 1–34. <https://doi.org/10.1007/s10533-004-0076-3>.
- Neville, J., Tessier, J.L., Morrison, I., Scarratt, J., Canning, B., Klironomos, J.N., 2002. Soil depth distribution of ecto- and arbuscular mycorrhizal fungi associated with *Populus tremuloides* within a 3-year-old boreal forest clear-cut. *Appl. Soil Ecol.* 19 (3), 209–216. [https://doi.org/10.1016/S0929-1393\(01\)00193-7](https://doi.org/10.1016/S0929-1393(01)00193-7).
- Nierop, K., Buurman, P., de Leeuw, J.W., 1999. Effect of vegetation on chemical composition of H horizons in incipient podzols as characterized by ^{13}C NMR and pyrolysis-GC/MS. *Geoderma* 90, 111–129. [https://doi.org/10.1016/s0016-7061\(98\)00095-0](https://doi.org/10.1016/s0016-7061(98)00095-0).
- Nierop, K.G.J., 1998. Origin of aliphatic compounds in a forest soil. *Org Geochem.* 29 (4), 1009–1016. [https://doi.org/10.1016/S0146-6380\(98\)00165-X](https://doi.org/10.1016/S0146-6380(98)00165-X).
- Oksanen, J., Guillaume Blanchet, F., Friendly, M., Kindt, R., Legendre, P., McGlinn, D., Minchin, P.R., O'Hara, R.B., Simpson, G.L., Solymos, P., Stevens, M.H.H., Szoecs, E., Wagner, H., 2018. vegan: Community Ecology Package.
- Öquist, M.G., Bishop, K., Grelle, A., Klemetsson, L., Köhler, S.J., Laudon, H., Lindroth, A., Ottosson Löfvenius, M., Wallin, M.B., Nilsson, M.B., 2014. The full annual carbon balance of boreal forests is highly sensitive to precipitation. *Environmental Science & Technology Letters* 1, 315–319. doi:10.1021/ez500169j.
- Otjen, L., Blanchette, R.A., 1985. Selective delignification of aspen wood blocks in vitro by three white rot basidiomycetes. *Appl. Environ. Microbiol.* 50, 568–572. <https://doi.org/10.1128/AEM.50.3.568-572.1985>.
- Palmroth, S., Holm Bach, L., Nordin, A., Palmqvist, K., 2014. Nitrogen-addition effects on leaf traits and photosynthetic carbon gain of boreal forest understory shrubs. *Oecologia* 175 (2), 457–470. <https://doi.org/10.1007/s00442-014-2923-9>.
- Patterson, S.L., Zak, D.R., Burton, A.J., Talhelm, A.F., Pregitzer, K.S., 2012. Simulated N deposition negatively impacts sugar maple regeneration in a northern hardwood ecosystem. *J. Appl. Ecol.* 49, 155–163. <https://doi.org/10.1111/j.1365-2664.2011.02090.x>.
- Persson, H.Å., 1983. The distribution and productivity of fine roots in boreal forests. *Plant Soil* 71 (1-3), 87–101. <https://doi.org/10.1007/BF02182644>.
- Pihl-Karlsson, G., Karlsson, P., Åkesson, C., Kronnäs, V., Hellsten, S., 2013. Krondroppsnätets övervakning av luftföroreningar i Sverige—mätningar och modellering. Stockholm, Sweden.
- Pisani, O., Frey, S.D., Simpson, A.J., Simpson, M.J., 2015. Soil warming and nitrogen deposition alter soil organic matter composition at the molecular-level. *Biogeochemistry* 123 (3), 391–409. <https://doi.org/10.1007/s10533-015-0073-8>.
- Poirier, N., Sohi, S.P., Gaunt, J.L., Mahieu, N., Randall, E.W., Powson, D.S., Evershed, R.P., 2005. The chemical composition of measurable soil organic matter pools. *Org Geochem.* 36 (8), 1174–1189. <https://doi.org/10.1016/j.orggeochem.2005.03.005>.
- R Core Team, 2018. R: A Language and Environment for Statistical Computing. R Foundation for Statistical Computing, Vienna, Austria.
- R Core Team, 2012. R: A Language and Environment for Statistical Computing. R Foundation for Statistical Computing, Vienna, Austria.
- Reay, D.S., Dentener, F., Smith, P., Grace, J., Feely, R.A., 2008. Global nitrogen deposition and carbon sinks. *Nat. Geosci.* 1 (7), 430–437. <https://doi.org/10.1038/ngeo230>.
- Rinkes, Z.L., Bertrand, I., Amin, B.A.Z., Grandy, A.S., Wickings, K., Weintraub, M.N., 2016. Nitrogen alters microbial enzyme dynamics but not lignin chemistry during maize decomposition. *Biogeochemistry* 128 (1-2), 171–186. <https://doi.org/10.1007/s10533-016-0201-0>.
- Saiz-Jimenez, C., 1994. Analytical Pyrolysis of Humic Substances: Pitfalls, Limitations, and Possible Solutions. *Environ. Sci. Technol.* 28 (11), 1773–1780. <https://doi.org/10.1021/es00060a005>.
- Sarkanen, K.V., Ludwig, C.H., 1971. Lignins: occurrence, formation, structure and reactions. Wiley, New York.
- Schellekens, J., Buurman, P., Pontevedra-Pombal, X., 2009. Selecting parameters for the environmental interpretation of peat molecular chemistry—A pyrolysis-GC/MS study. *Org Geochem.* 40 (6), 678–691. <https://doi.org/10.1016/j.orggeochem.2009.03.006>.
- Sebilo, M., Mayer, B., Nicolardot, B., Pinay, G., Mariotti, A., 2013. Long-term fate of nitrate fertilizer in agricultural soils. *Proc. Natl. Acad. Sci.* 110 (45), 18185–18189. <https://doi.org/10.1073/pnas.1305372110>.
- Sikora, L.J., Enkiri, N.K., 2001. Uptake of ^{15}N fertilizer in compost-amended soils. *Plant Soil* 235, 65–73. <https://doi.org/10.1023/A:1011855431544>.
- Smernik, R.J., 2005. Solid-state ^{13}C NMR spectroscopic studies of soil organic matter at two magnetic field strengths. *Geoderma* 125 (3-4), 249–271. <https://doi.org/10.1016/j.geoderma.2004.08.003>.
- Stankiewicz, B.A., van Bergen, P.F., Duncan, I.J., Carter, J.F., Briggs, D.E.G., Evershed, R.P., 1996. Recognition of chitin and protein in invertebrate cuticles using analytical pyrolysis/gas chromatography and pyrolysis/gas chromatography/mass spectrometry. *Rapid Commun. Mass Spectrom.* 10, 1747–1757. [https://doi.org/10.1002/\(SICI\)1097-0231\(199611\)10:14<1747::AID-RCM713>3.0.CO;2-H](https://doi.org/10.1002/(SICI)1097-0231(199611)10:14<1747::AID-RCM713>3.0.CO;2-H).
- Stark, S., Männistö, M.K., Eskelinen, A., 2014. Nutrient availability and pH jointly constrain microbial extracellular enzyme activities in nutrient-poor tundra soils. *Plant Soil* 383 (1-2), 373–385. <https://doi.org/10.1007/s11104-014-2181-y>.
- Stuczynski, T.I., McCarty, G.W., Reeves, J.B., Wright, R.J., 1997. Use of pyrolysis GC/MS for assessing changes in soil organic matter quality. *Soil Sci.* 162 (2), 97–105.
- Swathi, T.A., Rakesh, M., Premsai, B.S., Louis, T.S., William, T.K., Subhash, M.C., 2013. Chronic N-amended soils exhibit an altered bacterial community structure in Harvard Forest, MA, USA. *FEMS Microbiology Ecology* 83, 478–493. doi:10.1111/1574-6941.12009.
- Tarasov, D., Leitch, M., Fatehi, P., 2018. Lignin-carbohydrate complexes: properties, applications, analyses, and methods of extraction: a review. *Biotechnol. Biofuels* 11 (1). <https://doi.org/10.1186/s13068-018-1262-1>.
- Tegelaar, E.W., De Leeuw, J.W., Holloway, P.J., 1989. Some mechanisms of flash pyrolysis of naturally occurring higher plant polyesters. *J. Anal. Appl. Pyrol.* 15, 289–295. [https://doi.org/10.1016/0165-2370\(89\)85041-7](https://doi.org/10.1016/0165-2370(89)85041-7).
- Tian, D., Niu, S., 2015. A global analysis of soil acidification caused by nitrogen addition. *Environ. Res. Lett.* 10 (2), 024019. <https://doi.org/10.1088/1748-9326/10/2/024019>.
- Tolu, J., Gerber, L., Boily, J.-F., Bindler, R., 2015. High-throughput characterization of sediment organic matter by pyrolysis-gas chromatography/mass spectrometry and multivariate curve resolution: a promising analytical tool in (paleo)limnology. *Anal. Chim. Acta* 880, 93–102. <https://doi.org/10.1016/j.aca.2015.03.043>.
- Tolu, J., Rydberg, J., Meyer-Jacob, C., Gerber, L., Bindler, R., 2017. Spatial variability of organic matter molecular composition and elemental geochemistry in surface sediments of a small boreal Swedish lake. *Biogeosciences* 14 (7), 1773–1792. <https://doi.org/10.5194/bg-14-1773-2017-05194/bg-14-1773-2017-supplement>.
- van den Enden, L., Frey, S.D., Nadelhoffer, K.J., LeMoine, J.M., Lajtha, K., Simpson, M.J., 2018. Molecular-level changes in soil organic matter composition after 10 years of litter, root and nitrogen manipulation in a temperate forest. *Biogeochemistry* 141, 183–197. <https://doi.org/10.1007/s10533-018-0512-4>.
- Waldrop, M.P., Zak, D.R., 2006. Response of Oxidative Enzyme Activities to Nitrogen Deposition Affects Soil Concentrations of Dissolved Organic Carbon. *Ecosystems* 9 (6), 921–933. <https://doi.org/10.1007/s10021-004-0149-0>.
- Waldrop, M.P., Zak, D.R., Sinsabaugh, R.L., Gallo, M., Lauber, C., 2004. Nitrogen deposition modifies soil carbon storage through changes in microbial enzymatic activity. *Ecol. Appl.* 14 (4), 1172–1177. <https://doi.org/10.1890/03-5120>.
- Wang, J.-J., Bowden, R.D., Lajtha, K., Washko, S.E., Wurzbacher, S.J., Simpson, M.J., 2019. Long-term nitrogen addition suppresses microbial degradation, enhances soil carbon storage, and alters the molecular composition of soil organic matter. *Biogeochemistry* 142 (2), 299–313. <https://doi.org/10.1007/s10533-018-00535-4>.
- Wickland, K.P., Neff, J.C., 2008. Decomposition of soil organic matter from boreal black spruce forest: environmental and chemical controls. *Biogeochemistry* 87 (1), 29–47. <https://doi.org/10.1007/s10533-007-9166-3>.
- Winkler, A., Haumaier, L., Zech, W., 2005. Insoluble alkyl carbon components in soils derive mainly from cutin and suberin. *Org. Geochem.* 36 (4), 519–529. <https://doi.org/10.1016/j.orggeochem.2004.11.006>.
- Yang, Y., Luo, Y., Lu, M., Schädel, C., Han, W., 2011. Terrestrial C: N stoichiometry in response to elevated CO_2 and N addition: a synthesis of two meta-analyses. *Plant Soil* 343 (1-2), 393–400. <https://doi.org/10.1007/s11104-011-0736-8>.
- Ye, C., Chen, D., Hall, S.J., Pan, S., Yan, X., Bai, T., Guo, H., Zhang, Y.i., Bai, Y., Hu, S., Reynolds, H., 2018. Reconciling multiple impacts of nitrogen enrichment on soil

- carbon: plant, microbial and geochemical controls. *Ecol. Lett.* 21 (8), 1162–1173. <https://doi.org/10.1111/ele.2018.21.issue-810.1111/ele.13083>.
- Zak, D.R., Argiroff, W.A., Freedman, Z.B., Upchurch, R.A., Entwistle, E.M., Romanowicz, K.J., 2019. Anthropogenic N deposition, fungal gene expression, and an increasing soil carbon sink in the Northern Hemisphere. *Ecology* 100 (10). <https://doi.org/10.1002/ecy.v100.1010.1002/ecy.2804>.
- Zak, D.R., Freedman, Z.B., Upchurch, R.A., Steffens, M., Kögel-Knabner, I., 2017. Anthropogenic N deposition increases soil organic matter accumulation without altering its biochemical composition. *Glob. Change Biol.* 23, 933–944. <https://doi.org/10.1111/gcb.13480>.